Plant Cell Advance Publication. Published on September 18, 2018, doi:10.1105/tpc.18.00547

RESEARCH ARTICLE

A MPK3/6-WRKY33-ALD1-Pipecolic acid Regulatory Loop Contributes to Systemic Acquired Resistance

Yiming Wang[a], Stefan Schuck[b,c], Jingni Wu[a,1], Ping Yang[a,2], Anne-Christin Döring[b], Jürgen Zeier[b,c,*], and Kenichi Tsuda[a,*]

[a]Department of Plant Microbe Interactions, Max Planck Institute for Plant Breeding Research, Carl-von-Linné Weg 10, 50829, Cologne, Germany.
[b]Department of Molecular Ecophysiology of Plants, Heinrich Heine University Düsseldorf, Universitätsstraße 1, 40225 Düsseldorf, Germany
[c]Cluster of Excellence on Plant Sciences (CEPLAS), Heinrich Heine University, Universitätsstraße 1, 40225 Düsseldorf, Germany

Present address:
[1] Shanghai Institute of Plant Physiology and Ecology, Chinese Academy of Sciences, Shanghai 200032, China
[2] Institute of Crop Sciences, Chinese Academy of Agricultural Sciences, Beijing 100081, China.

[*]**To whom correspondence should be addressed:**
Kenichi Tsuda (tsuda@mpipz.mpg.de) and Jürgen Zeier (Juergen.Zeier@uni-dusseldorf.de)

Short title: MPK3/6-WRKY33-ALD1 loop for Pip-mediated SAR

One sentence summary: A positive feedback loop consisting of MPK3/6, WRKY33, ALD1, and pipecolic acid regulates local immune amplification contributing to systemic acquired resistance in *Arabidopsis thaliana.*

The authors responsible for distribution of materials integral to the findings presented in this article in accordance with the policy described in the Instructions for Authors (www.plantcell.org) are: Kenichi Tsuda (tsuda@mpipz.mpg.de) and Jürgen Zeier (Juergen.Zeier@uni-dusseldorf.de).

ABSTRACT

Plants induce systemic acquired resistance (SAR) upon localized exposure to pathogens. Pipecolic acid (Pip) production via AGD2-LIKE DEFENSE RESPONSE PROTEIN 1 (ALD1) is key for SAR establishment. Here, we report a positive feedback loop important for SAR induction in *Arabidopsis thaliana*. We showed that local activation of the MAP kinases MPK3 and MPK6 is sufficient to trigger Pip production and mount SAR. Consistent with this, mutations in *MPK3* or *MPK6* led to compromised Pip accumulation upon inoculation with the bacterial pathogen *Pseudomonas syringae* pv. *tomato* DC3000 (*Pto*) AvrRpt2, which triggers strong sustained MAPK activation. By contrast, *P. syringae* pv. *maculicola* (*Pma*) and *Pto,* which induce transient MAPK activation, trigger Pip biosynthesis and SAR independently of MPK3/6. *ALD1* expression, Pip accumulation, and SAR were compromised in mutants defective in the

MPK3/6-regulated transcription factor WRKY33. Chromatin immunoprecipitation showed that WRKY33 binds to the *ALD1* promoter. We found that Pip triggers activation of MPK3 and MPK6 and that MAPK activation after *Pto* AvrRpt2 inoculation is compromised in *wrky33* and *ald1* mutants. Collectively, our results reveal a positive regulatory loop consisting of MPK3/MPK6, WRKY33, ALD1, and Pip in SAR induction and suggest the existence of distinct SAR activation pathways that converge at the level of Pip biosynthesis.

INTRODUCTION

Plants have evolved two types of innate immune system to deal with attacks by microbial pathogens: cell surface receptor-mediated immunity (pattern-triggered immunity or PTI) and intracellular receptor-mediated immunity (effector-triggered immunity or ETI) (Jones and Dangl, 2006; Tsuda and Katagiri, 2010). PTI is induced by the recognition of microbe-associated molecular patterns (MAMPs) by pattern recognition receptors (PRRs) on the plasma membrane, which are receptor-like kinases (RLKs) or receptor-like proteins (RLPs) (Jones and Dangl, 2006; Boutrot and Zipfel, 2017; Yu et al., 2017). For instance, the bacterial MAMP flg22, a part of bacterial flagellin, is recognized by FLAGELLIN-SENSITIVE2 (FLS2) and the co-receptors BRI1-ASSOCIATED RECEPTOR KINASE1 (BAK1) and BAK1-LIKE1 (BKK1) in *Arabidopsis thaliana* (Gomez-Gomez and Boller, 2000; Zipfel et al., 2004; Chinchilla et al., 2007; Roux et al., 2011). ETI is triggered by recognition of virulence factors such as bacterial type III effectors (T3Es) with which pathogens subvert plant immunity in susceptible plants by mostly nucleotide-binding/leucine-rich repeat (NLR) receptors (Jones and Dangl, 2006; Cui et al., 2015; Tran et al., 2017; Zhang et al., 2017). For instance, AvrRpt2 and AvrRpm1 are T3Es of the bacterial pathogen *Pseudomonas syringae* whose virulence actions are recognized by the NLR receptors RESISTANCE TO P. SYRINGAE (RPS2) and RESISTANCE TO P. SYRINGAE PV MACULICOLA 1 (RPM1), respectively, in *A. thaliana* (Mackey et al., 2002; Axtell and Staskawicz, 2003; Mackey et al., 2003).

PTI and ETI share signaling components such as the phytohormone salicylic acid (SA) and mitogen-activated protein kinases (MAPKs) (Tsuda and Katagiri, 2010). SA regulates a major portion of plant immunity against biotrophic and hemibiotrophic pathogens such as *P. syringae* via the central regulator/receptor of SA signaling

NONEXPRESSER OF PR GENES 1 (NPR1) (Delaney et al., 1994; Cao et al., 1997; Wu et al., 2012; Pajerowska-Mukhtar et al., 2013; Ding et al., 2018). *A. thaliana* MAPKs, MPK3 and MPK6, positively contribute to immunity against a wide range of pathogens via phosphorylation of substrates in a partially redundant manner (Beckers et al., 2009; Meng and Zhang, 2013; Xu et al., 2016; Ding et al., 2018). For instance, the WRKY family transcription factor WRKY33, a direct phosphorylation target of MPK3 and MPK6, is necessary for MPK3 and MPK6-mediated production of the phytoalexin camalexin and the phytohormone ethylene (Mao et al., 2011; Li et al., 2012).

Plants systemically induce broad spectrum resistance called systemic acquired resistance (SAR) upon localized exposure to pathogens (Fu and Dong, 2013). Although the identity of the mobile signal that relays local immune activation for SAR activation in systemic tissues is still under debate, several molecules have been implicated in the establishment of SAR such as methyl salicylate (Park et al., 2007), dehydroabietinal (Chaturvedi et al., 2012), glycerol-3-phosphate (Chanda et al., 2011), azelaic acid (Jung et al., 2009), and pipecolic acid (Pip) (Navarova et al., 2012). Pip is a Lys catabolite that is present ubiquitously in the plant kingdom and accumulates to high levels in *P. syringae*-inoculated leaves and in distant, uninfected leaves at the onset of SAR (Navarova et al., 2012; Zeier, 2013). Pip is synthesized by AGD2-LIKE DEFENSE RESPONSE PROTEIN 1 (ALD1) and SAR-DEFICIENT4 (SARD4) (Navarova et al., 2012; Ding et al., 2016; Hartmann et al., 2017). The biosynthesis of Pip is fully dependent on ALD1 which functions as an α-L-Lys aminotransferase and generates the biosynthetic intermediate 2,3-dehydropipecolic acid (2,3-DP). 2,3-DP is subsequently reduced to Pip by SARD4 and another reductase activity (Navarova et al., 2012; Ding et al., 2016; Hartmann et al., 2017). Pip is further converted by Flavin-dependent monooxygenase1 (FMO1) to N-hydroxypipecolic acid (NHP), which is a critical component for SAR activation (Chen et al., 2018; Hartmann et al., 2018). The accumulation of Pip and NHP in pathogen-inoculated plants is required for SAR, and exogenous application of Pip or NHP is sufficient to systemically trigger immunity (Navarova et al., 2012; Vogel-Adghough et al., 2013; Chen et al., 2018; Hartmann et al., 2018). The expression of *ALD1* and *SARD4* is positively regulated by the transcription factors SAR-DEFICIENT 1 (SARD1) and CALMODULIN BINDING PROTEIN 60g (CBP60g) (Sun et al., 2015; Sun et al., 2017), which also regulate expression of *SALICYLIC ACID INDUCTION DEFICIENT 2* (*SID2*), encoding an SA biosynthesis enzyme that is required for SA production upon pathogen infection in *A.*

thaliana (Wildermuth et al., 2001; Zhang et al., 2010; Wang et al., 2011). It was recently found that expression of *SARD1* and *CBP60g* is regulated by the transcription factors TGA1, TGA4, and WRKY70 (Sun et al., 2017; Zhou et al., 2017).

Although SA is not the mobile signal for SAR, it contributes to SAR (Vernooij et al., 1994; Lawton et al., 1995; Park et al., 2007). SA is required for SAR in systemic leaves but not local infected leaves of tobacco (*Nicotiana tabacum*) plants (Vernooij et al., 1994). Furthermore, SA contributes to SAR signal amplification together with ALD1 and FMO1 in *A. thaliana* systemic leaves, exemplifying the important role of SA in systemic tissues for SAR (Bernsdorff et al., 2016).

Previous research showed that MPK3 and MPK6 can regulate immune responses redundantly with SA signaling when they are activated in a sustained manner but not in a transient manner (Tsuda et al., 2013). Artificial sustained activation of MPK3 and MPK6 triggered by dexamethasone (DEX)-induced expression of $MKK4^{DD}$, a constitutively active form of MAPK kinase 4 that can phosphorylate the downstream MPK3 and MPK6 (Ren et al., 2002; Tsuda et al., 2013), was sufficient to induce expression of SA-responsive genes without *SID2* (Nawrath and Metraux, 1999; Wildermuth et al., 2001; Tsuda et al., 2013). These results suggest that MPK3 and MPK6 contribute to SAR. Indeed, it has been shown that *MPK3* is required for SAR triggered by local infection with *Pto* AvrRpt2 (Beckers et al 2009). However, the molecular mechanism by which the MAPK signaling regulate the establishment of SAR is yet unknown.

Here, we show that a positive regulatory loop for local Pip accumulation contributes to SAR in *A. thaliana*. Sustained MAPK activation induces *ALD1* expression via WRKY33 to increase local Pip accumulation. Pip application triggers activation of MPK3 and MPK6. MAPK activation during *Pto* AvrRpt2 infection is compromised in *wrky33*, *ald1*, and *fmo1* mutant plants. These results suggest that the regulatory loop consisting of MPK3/MPK6, WRKY33, ALD1, and Pip in local leaves plays a critical role in the establishment of SAR when the MAPKs are locally activated in a sustained manner.

RESULTS

Local MAPK activation triggers SAR

SA application triggers SAR (Lawton et al., 1995), and MPK3 and MPK6 regulate immune responses redundantly with SA, when they are activated in a sustained manner (Tsuda et al., 2013). Therefore, we hypothesized that sustained MPK3/MPK6 activation in local leaves triggers SAR in systemic leaves of *A. thaliana*. Transgenic plants expressing MKK4^{DD} (MKK4^{DD}) under the control of a DEX-inducible promoter (Ren et al., 2002; Tsuda et al., 2013) were employed to investigate the effect of localized MAPK activation. DEX treatment induced the expression of defense marker genes *PATHOGENESIS-RELATED 1* (*PR1*) and *FLG22-INDUCED RECEPTOR-LIKE KINASE 1* (*FRK1*) in MKK4^{DD} plants as well as in MKK4^{DD} *sid2* (Figure 1A). Interestingly, expression of *ALD1* was also induced by activation of MPK3 and MPK6 in both MKK4^{DD} and MKK4^{DD} *sid2* plants (Figure 1A), pointing to a role of MPK3/MPK6 in SAR establishment without SA. Indeed, we observed that SAR is triggered in MKK4^{DD} and to a lesser extent, MKK4^{DD} *sid2* plants after DEX treatment in local leaves (Figure 1B), whereas no SAR was observed after DEX treatment in Col-0, *sid2*, and transgenic plants harboring DEX-inducible GUS (GVG:GUS) (Figure 1B). We did not detect expression of the *MKK4^{DD}* or *GUS* transgene in systemic leaves of MKK4^{DD} or GVG:GUS plants, respectively, after local DEX application, suggesting that DEX itself did not translocate from local leaves to systemic leaves (Supplemental Figure 1A and 1B). Thus, local MAPK activation appeared to trigger SAR. Consistent with this, expression of *PR1*, *FRK1*, and *ALD1*, and SAR, were induced in both Col-0 and *sid2* plants upon infection with *Pto* AvrRpt2 (Figure 1C and 1D), which triggers strong sustained MAPK activation (Tsuda et al., 2013).

MAPK-mediated SAR requires *ALD1*

Next, we tested whether known SAR components are required for the MAPK activation-triggered SAR. MKK4^{DD} plants were crossed with *fmo1*, *ald1*, and *npr1* mutants, in which SAR was shown to be robustly compromised in various conditions (Cao et al., 1997; Mishina and Zeier, 2006; Bernsdorff et al., 2016; Hartmann et al., 2018). SAR assay after local DEX application showed that *FMO1*, *ALD1*, and *NPR1*, but not *SID2* are required for the MAPK-mediated SAR (Figure 2A). Immunoblotting of MKK4^{DD}-flag, MPK3, and MPK6 showed that the MKK4^{DD} inducible system is intact and MPK3 and MPK6 protein accumulation remain unaltered in these genetic backgrounds (Figure 2B). Notably, MAPK activation was compromised in *ald1* and

fmo1 backgrounds (Figure 2B), suggesting that MAPK activation triggered by MKK4^{DD} requires the Pip pathway. Consistent with this, we found that *FMO1*, *ALD1*, and *NPR1* are required for SAR triggered by local *Pto* AvrRpt2 infection (Supplemental Figure 2A). MAPK-mediated *ALD1* (Figure 1A) and *FMO1* induction (Figure 4A) prompted us to test whether MAPK activation triggers increased Pip and NHP accumulation in local leaves. Indeed, Pip and NHP accumulation was increased in local leaves of MKK4^{DD} plants after DEX application (Figure 2C). These results suggest that MAPK activation induces *ALD1* and *FMO1* expression to increase local Pip and NHP accumulation, thereby contributing to SAR. Considering that Pip is metabolized to NHP by FMO1 and that Pip-induced responses require *FMO1* (Chen et al., 2018; Hartmann et al., 2018), this indicates that NHP is the key signaling molecule in MAPK-mediated SAR. Consistent with previous reports (Ren et al., 2008), accumulation of the phytoalexin camalexin also increased (Supplemental Figure 1C).

MPK3 and MPK6 positively regulate Pip accumulation upon infection with *Pto* AvrRpt2

We investigated the genetic requirement of *MPK3* or *MPK6* for the establishment of SAR. We first employed two systems to trigger SAR, local infection with *Pto* or *Pto* AvrRpt2, which activates MPK3 and MPK6 in a transient or sustained manner, respectively (Tsuda et al., 2013). Upon local infection with *Pto*, SAR was detected in Col-0, *mpk3*, and *mpk6* but not *sid2*, *mpk3 sid2*, and *mpk6 sid2* (Supplemental Figure 3A), suggesting that SA is required for *Pto*-triggered SAR. In contrast, upon local infection with *Pto* AvrRpt2, SAR was observed in Col-0, *mpk3*, *mpk6*, and *sid2* but not in *mpk3 sid2* and *mpk6 sid2* (Figure 3A). *Pto* AvrRpt2-triggered induction of *ALD1* and *FMO1* in local leaves was compromised in *mpk3, mpk6, mpk3 sid2,* and *mpk6 sid2*, but not in *sid2* (Figure 3B), pointing to the positive roles of MPK3 and MPK6 for local *ALD1* and *FMO1* expression. As previously reported (Tsuda et al., 2013), *PR1* expression was redundantly regulated by the MAPKs and SA (Figure 3B). Local Pip accumulation was decreased in *mpk3* and *mpk6* compared to Col-0 and in *mpk3 sid2* and *mpk6 sid2* compared to *sid2* (Figure 3C), indicating positive roles of *MPK3* and *MPK6* in Pip accumulation. Pip accumulation was elevated in *sid2* compared with Col-0 and in *mpk3 sid2* and *mpk6 sid2* compared to *mpk3* and *mpk6*, suggesting that SA negatively regulates Pip accumulation (Figure 3C). Curiously, *mpk3 sid2* and *mpk6*

sid2 showed Col-0-like Pip accumulation yet compromised SAR (Figure 3A and 3C). Thus, the amount of locally accumulating Pip alone does not explain the observed SAR phenotypes.

MAPK-mediated Pip accumulation and SAR are compromised in *wrky33*

The transcription factor WRKY33 regulates defense responses against a wide range of pathogens (Zheng et al., 2006; Liu et al., 2015; Liao et al., 2016; Liu et al., 2017) and is activated by MPK3 and MPK6 via phosphorylation (Mao et al., 2011). Therefore, we hypothesized that WRKY33 regulates MAPK-mediated *ALD1* expression and Pip accumulation. Consistent with our hypothesis, levels of local *ALD1* expression as well as *PR1* and *FMO1* and Pip accumulation after MAPK activation were reduced in *wrky33* (Figure 4A and 4B) while $MKK4^{DD}$ protein was induced after DEX treatment similarly to wild type background (Figure 2B). MAPK-mediated SAR was also partially but significantly reduced in $MKK4^{DD}$ *wrky33* compared to $MKK4^{DD}$ plants (Figure 4C), suggesting that *WRKY33* mediates MAPK-regulated SAR via *ALD1* induction. Consistent with this, the levels of *ALD1* expression as well as *PR1* and *FMO1*, Pip accumulation, and SAR were significantly reduced in *wrky33* upon local *Pto* AvrRpt2 infection (Figure 4D and 4E). Similar to Figure 3, *wrky33 sid2* showed Col-0-like Pip accumulation but compromised SAR and Pip accumulation was elevated in *sid2* compared with Col-0 and in *wrky33 sid2* compared to *wrky33* (Figure 4E and 4F). Moreover, the *Pto*-induced SAR fully depended on functional *WRKY33* as well (Supplemental Figure 3B).

SAR triggered by multiple stimuli converges at WRKY33, ALD1, and FMO1

To better understand the roles of the MAPK-WRKY33 and SA pathways in SAR induced by different stimuli, we also investigated local Pip accumulation and SAR triggered by local infection with the bacterial strain *Pseudomonas syringae* pv. *maculicola* ES4326 (*Pma*). *Pma* inoculation induces robust SAR in *A. thaliana* and has been used extensively to investigate the underlying molecular mechanisms (Mishina and Zeier, 2006; Liu et al., 2011; Bernsdorff et al., 2016; Hartmann et al., 2018). Similar to *Pto* but in contrast to *Pto* avrRpt2 or *Pma* expressing avrRpm1, *Pma* did not trigger sustained MAPK activation in inoculated leaves (Supplemental Figure 4A). Consistent

with previous findings (Bernsdorff et al., 2016), a weak but significant SAR response was observed in *sid2* after *Pma* inoculation, as well as in *mpk3 sid2* (Figure 5A). Thus, similar to SAR triggered by local *Pto* infection, the *Pma*-triggered SAR establishment was predominantly dependent on SA (Figure 5A). In addition, *Pma* inoculation triggered SAR in both *mpk3* and *mpk6* to nearly same levels with Col-0 wild type (Figure 5A). This was accompanied with wild type-like accumulation of Pip in the locally inoculated and systemic leaves of both *mpk3* and *mpk6* mutants (Figure 5C). The *Pma*-induced biosynthesis of NHP and camalexin, however, was specifically reduced in *mpk3* (Figure 5C, Supplemental Figure 4B). Moreover, SAR triggered by *Pma* was attenuated in *wrky33* plants (Figure 5B), and local Pip and NHP, as well as systemic Pip accumulation was reduced in *wrky33* upon local *Pma* infection (Figure 5C).

Thus, the absence of just *MPK3* or *MPK6* appears to have only minor effects on Pip accumulation and SAR when local MAPK activation is not sustained, as is the case for *Pma*- and *Pto*-inoculation. Nevertheless, *WRKY33* plays common roles in SAR triggered by multiple pathogen stimuli irrespective of the MAPK activation kinetics in local leaves (Figure 4F and 5B; Supplemental Figure 4B), suggesting that WRKY33 activity may also be regulated by other factors than the MAPKs. The growth assays with the different bacterial strains also indicate a WRKY33-independent signaling branch to SAR that is activated after *Pma* inoculation and induces a partial SAR. Consistent with previous reports (Návarová et al., 2012, Hartmann et al., 2018), these different signaling pathways leading to SAR induction converge at *ALD1* (Figure 2A, Supplemental Figure 2)

WRKY33 binds to the *ALD1* promoter

Compromised *ALD1* expression and Pip accumulation triggered by MAPK activation in *wrky33* (Figure 4A and 4B), suggests WRKY33 directly regulates *ALD1* expression. Indeed, three W-boxes, the binding motif of WRKYs, were found in the *ALD1* promoter (Figure 6A). Therefore, we investigated WRKY33 binding to these W-boxes by chromatin immunoprecipitation followed by quantitative PCR (ChIP-qPCR) in *Pwrky33:WRKY33-HA* plants (Liu et al., 2015). Accumulation of WRKY33 was detected from 6 h post infiltration with *Pto* AvrRpt2 (Figure 6B). We detected strong enrichment of *Pwrky33:WRKY33-HA* for W-box 2/3 compared to Col-0 control but not for W-box 1 (Figure 6C). This result is consistent with the large scale ChIP sequencing

study showing that WRKY33 binds to W-box 2/3 but not W-box 1 in the *ALD1* promoter (Birkenbihl et al., 2017). Thus, WRKY33 appears to regulate *ALD1* expression via direct binding to the W-box 2/3 in the *ALD1* promoter.

Pip triggers MAPK activation and *ALD1* is required for sustained MAPK activation upon *Pto* AvrRpt2 infection

Since it is known that defense activation often results in growth retardation (Huot et al., 2014), we investigated whether Pip affects root growth. We found that Pip triggers root growth retardation although its effect was weaker than that of flg22, a MAMP and known inducer of root growth retardation (Chinchilla et al., 2007) (Figure 7A). Root growth retardation triggered by Pip as well as flg22 was abolished in *bak1 bkk1*, which is deficient in the co-receptors of some membrane-localized MAMP receptors (Figure 7A). Moreover, Pip-triggered root growth retardation was not observed with the isomeric and non-active form of Pip (D-Pip) but the active form of Pip (L-Pip) (Navarova et al., 2012) (Figure 7A). We then explored the possibility that Pip triggers MAPK activation. Strikingly, L-Pip but not D-Pip triggered transient activation of MPK3 and MPK6 dependently on *BAK1 BKK1* (Figure 7B; Supplemental Figure 5). These results may suggest that Pip is sensed by plant membrane-localized receptor(s) to trigger MAPK activation.

Since the MAPK-WRKY33-ALD1 pathway positively regulated Pip accumulation under sustained MAPK activation conditions (Figure 2B and 4B), these results also suggest the existence of a regulatory loop for defense amplification. If this holds true, MAPK activation should be compromised in mutant plants deficient in this regulatory loop. Indeed, we observed that sustained local MAPK activation triggered by *Pto* AvrRpt2 infection was compromised in *wrky33, ald1,* and *fmo1* (Figure 7C and 7D), supporting the regulatory loop consisting of MPK3/MPK6, WRKY33, ALD1, FMO1, and Pip/NHP for SAR establishment under induction conditions involving local sustained MAPK activation. This amplification loop might be circumvented if Pip levels were elevated in the plant to high levels by exogenous treatment. To test this hypothesis, we supplemented plants with a dose of 10 µmol Pip, a treatment known to result in Pip augmentation in leaves to SAR-like levels and in the induction of systemic immunity (Navarova et al., 2012; Vogel-Adghough et al., 2013; Bernsdorff et al., 2016), and performed *Pma* growth assay in Col-0, *mpk3*, *mpk6*, and *wrky33* plants. We observed

significant Pip-induced resistance against *Pma* in Col-0, as well as *mpk3*, *mpk6,* and *wrky33* (Figure 7E), indicating that the MPK3/MPK6- and WRKY33-based regulatory loop can be bypassed by high amounts of Pip. However, consistent with our observation that Pip-induced root growth inhibition and MAPK activation were compromised in *bak1 bkk1* mutant plants (Figure 7A and 7B), Pip-induced immunity against *Pma* required *BAK1 BKK1* (Figure 7E).

DISCUSSION

In this study, we identified a regulatory loop for Pip accumulation upon local pathogen exposure which contributes to SAR in *A. thaliana* (Figure 7F). Our results and previous publications demonstrate that (1) Local MAPK activation triggers SAR; (2) Sustained MAPK activation induces *ALD1* and *FMO1* expression as well as Pip and NHP accumulation; (3) Direct activation of WRKY33 by MPK3 and MPK6 was previously shown (Mao et al., 2011); (4) WRKY33 directly regulates *ALD1* expression; (5) MAPK-mediated SAR is compromised in *wrky33, ald1*, and *fmo1* mutant plants; (6) Pip triggers MAPK activation; (7) Sustained MAPK activation triggered by *Pto* AvrRpt2 is compromised in *wrky33*, *ald1*, and *fmo1* mutants. Thus, the positive regulatory loop consisting of MPK3/MPK6, WRKY33, ALD1, FMO1, and Pip/NHP contributes to the establishment of SAR triggered by local sustained MAPK activation.

The SAR processes can be divided into three steps; local immune activation, information relay from local to systemic tissues by mobile signal(s), and defense activation and priming in systemic tissues (Jung et al., 2009; Shah and Zeier, 2013). In this study, we focused on local immune activation important for SAR establishment. We showed that artificial local activation of MPK3 and MPK6 by the $MKK4^{DD}$ system is sufficient to trigger SAR (Figure 1). Genetic requirement of *MPK3* and *MPK6* for SAR was also detected when SAR is activated by local *Pto* AvrRpt2 infection, which triggers sustained MAPK activation (Figure 3). In contrast, SAR predominantly depends on SA when it is activated by local infection with *Pto* and *Pma*, both of which do not trigger sustained MAPK activation [Figure 5A; Supplemental Figure 3A; Supplemental Figure 4A; (Tsuda et al., 2013)]. Thus, the regulatory loop for SAR identified in this study may kick in and play critical roles in SAR when local MAPK activation is sustained.

ALD1 is commonly required for SAR triggered by local infection with *Pma* and *Pto* AvrRpt2 and by local MAPK activation as well as for systemic immunity induced by β-aminobutyric acid and azelaic acid (Figure 2A; Supplemental Figure 2) (Zimmerli et al., 2000; Jung et al., 2009; Navarova et al., 2012). ALD1- and FMO1-mediated Pip and NHP production, respectively, are highly induced during immunity (Navarova et al., 2012; Hartmann et al., 2017; Hartmann et al., 2018). Thus, the regulation of pathogen-induced *ALD1* and *FMO1* expression is crucial for SAR. We showed that WRKY33 positively regulates *ALD1* via its direct binding to the *ALD1* promoter to increase Pip accumulation (Figure 6). Induction of *ALD1* expression and Pip accumulation was not totally compromised in *wrky33* (Figure 4A and 4B), suggesting that other transcription factors also contribute to *ALD1* expression. Indeed, the transcription factors SARD1 and CBP60g directly regulate expression of *ALD1* as well as *SARD4* (Sun et al., 2015; Sun et al., 2017). *SARD4* encodes the dehydropipecolate reductase enzyme that reduces ALD1-produced 2,3-dehydropipecolic acid to Pip (Ding et al., 2016; Hartmann et al., 2017). More recently, it was shown that transcription factors TGA1 and TGA4 directly regulate the expression of *SARD1* and *CBP60g* and that Pip accumulation upon *Pma* infection is significantly reduced but not abolished in *tga1 tga4* and *sard1 cbp60g* mutants (Sun et al., 2017). Furthermore, SAR was abolished in *wrky33* when it is activated by local *Pto* infection irrespective to modes of MAPK activation (Figure 4 and Supplemental Figure 3B), whereas SAR activated by local *Pma* infection was attenuated but not fully abolished in *wrky33* (Figure 5B). These results suggest that both TAG1/TAG4-SARD1/CBP60g and WRKY33 regulate Pip accumulation and SAR triggered by local *Pma* infection while WRKY33 is the major regulator of SAR triggered by local *Pto* infection. Our study thus indicates the existence of distinct branches of SAR signaling that are differentially activated by different pathogen types. These signaling branches converge at *ALD1* and Pip production (Figure 7F). SAR induction also depends on *FMO1* for both MAPK activating *Pto* AvrRpt2 and non-activating *Pma* (Supplemental Figure 2) (Navarova et al., 2012), supporting the finding that Pip to NHP conversion by FMO1 is a critical step for SAR activation (Hartmann et al., 2018).

SA is required for SAR in systemic leaves but not local infected leaves of tobacco plants (Vernooij et al., 1994). Furthermore, SA contributes to SAR signal amplification together with ALD1 and FMO1 in *A. thaliana* systemic leaves (Bernsdorff et al., 2016). These results suggest that SA is an important component for SAR in systemic tissues but not local infected tissues. Previous results indicate that the SA-

deficient *sid2* mutant strongly overproduces NHP upon *Pma* infection, suggesting that SA negatively modulates levels of NHP (Hartmann et al., 2018). Similarly, we found here that SA acts as a negative regulator of *Pto AvrRpt2*-triggered local Pip accumulation (Figure 3C and 4E). This elevated Pip accumulation appears to be sufficient for *Pto* AvrRpt2-triggered SAR in the absence of SID2-produced SA (Figure 3A and 3C). However, *mpk3 sid2* and *mpk6 sid2*, which accumulates wild type levels of Pip in local leaves, did not trigger SAR after *Pto* AvrRpt2 infection (Figure 3A and 3C). One explanation for these observations is that elevated Pip/NHP levels but not wild type levels of Pip in local leaves are sufficient for SAR signal amplification in systemic leaves without SA. Thus, the strength of SAR appears to be determined by activities of local Pip/NHP pathway and systemic SA pathway. Interestingly, WRKY33 negatively regulates SA accumulation and signaling (Birkenbihl et al., 2012; Liu et al., 2015; Birkenbihl et al., 2017). Consistent with this, we found that compared with wild type plants, *wrky33* plants are more resistant against *Pma*, which is sensitive to SA-mediated immunity (Figure 5B). Thus, WRKY33 is a negative regulator of local defense via SA suppression and a positive regulator of SAR via Pip accumulation, exemplifying that regulations of local immunity and SAR are tightly linked.

Pip-triggered MAPK activation, root-growth inhibition, and Pip-induced SAR required *BAK1* and *BKK1* (Figure 7A, 7B, and 7E). BAK1 and BKK1 belong to the SOMATIC EMBRYOGENESIS RECEPTOR KINASEs (SERKs) that function as co-receptors for the recognition of multiple MAMPs as well as plant-derived damage-associated molecular patterns (DAMPs) on the plasma membrane (Chinchilla et al., 2007; Heese et al., 2007; Shan et al., 2008; Krol et al., 2010). The co-receptors BAK1 and BKK1 function with receptors belonging to RLKs or RLPs. Therefore, it is tempting to speculate that Pip or perhaps a Pip-derived product is sensed by RLKs or RLPs together with BAK1/BKK1, thereby triggering MAPK activation as described for flg22 recognition by FLS2 (Asai et al., 2002; Beckers et al., 2009). Recently, an NHP-hexose conjugate that accumulates dependently on *ALD1* and *FMO1* in *Pma*-inoculated leaves was detected in *A. thaliana* (Hartmann and Zeier, 2018). Forward/reverse genetic screens and genome-wide association analysis using diverse *A. thaliana* accessions might help to identify receptor(s) for Pip, NHP, or further NHP derivative(s) such as NHP-hexose, which may function as mobile metabolites involved in SAR long-distance signaling (Chen et al., 2018; Hartmann and Zeier, 2018). In *A. thaliana*, the DAMP receptors PEPR1 and PEPR2 recognize endogenous PROPEP-derived Pep

epitopes that activate immunity and function together with BAK1/BKK1 (Boller and Felix, 2009; Yamaguchi et al., 2010; Yamada et al., 2016). Interestingly, mutant plants deficient in *PEPR1* and *PEPR2* showed compromised SAR phenotypes triggered by local infection with *Pto* AvrRpm1 that triggers strong sustained MAPK activation (Ross et al., 2014). Likewise, application of Pep epitopes activates immune responses such as MAPK activation (Yamada et al., 2016). Thus, the SAR inducer Pip and the DAMPs Pep epitopes are both endogenously produced in plants and activate immunity and SAR, which renders the difference of DAMPs and SAR-related molecules ambiguous. Further research will be required to fully establish the difference and similarity between DAMPs and SAR inducers.

Pip triggers transient activation of MPK3 and MPK6 (Figure 7B and Supplemental Figure 5) yet *ALD1* and *FMO1* contribute to sustained MAPK activation after *Pto* AvrRpt2 infection (Figure 7C). One explanation for this is that sustained MAPK activation is achieved by multiple signal inputs including Pip/NHP and others. Alternative but not exclusive explanation is that Pip/NHP triggers transient activation of the MAPKs in different cells at different time points, resulting in sustained MAPK activation in local infected leaves. Measuring the temporal dynamics of the MAPK activities at the single cell resolution would help solve this issue.

The observation that MAPK activation triggered by $MKK4^{DD}$ requires *ALD1* and *FMO1* (Figure 2B) was rather surprising to us because $MKK4^{DD}$ would be able to directly phosphorylate MPK3 and MPK6 without other components. However, this suggests that $MKK4^{DD}$ requires additional components whose activity depends on Pip/NHP to achieve sustained activation of MPK3 and MPK6 in plants. We speculate that Pip/NHP may condition the proper formation of MKK4DD-MPK3/MPK6 complex through, for instance, affecting the subcellular localization of $MKK4^{DD}$, MPK3, and MPK6. Alternatively, $MKK4^{DD}$ triggers initial phosphorylation of MPK3 and MPK6, which then triggers sustained activation of MPK3 and MPK6 dependently on Pip/NHP. Recent work showed that MPK6 phosphorylates the upstream MAPK kinase kinase MAPKKK5 to enhance activation of MPK3 and MPK6 (Bi et al., 2018). Thus, Pip/NHP signaling may ensure, for instance, expression of *MAPKKK5* and this positive feedback mechanism may be required for $MKK4^{DD}$-triggered sustained activation of MPK3 and MPK6. Nevertheless, this speculation needs to be experimentally tested.

MATERIALS AND METHODS

Plant materials and growth conditions

Arabidopsis thaliana plants were grown in a chamber at 22ºC with a 10 h light (white fluorescence lamps) period and 60% relative humidity. The *A. thaliana* accession Col-0 was used as the wild-type. *A. thaliana* mutants and transgenic lines, *sid2-2* (Wildermuth et al., 2001), *mpk3-1* (Wang et al., 2007), *mpk6-2* (Liu and Zhang, 2004), *mpk3-1 sid2-2*, *mpk6-2 sid2-2* (Tsuda et al., 2013), *ald1-T2* (Mishina and Zeier, 2006), *fmo1-1* (Navarova et al., 2012), *npr1-1* (Cao et al., 1997), *wrky33-2* (Zheng et al., 2006), *Pwrky33:WRKY33-HA* (Liu et al., 2015), MKK4^{DD}, MKK4^{DD} *sid2* (Ren et al., 2002), MKK4^{DD} *npr1* (Tsuda et al., 2013), and *rpm1-3 rps2 101C* (Belkhadir et al., 2004) were previously described. The MKK4^{DD} *fmo1*, MKK4^{DD} *ald1*, and MKK4^{DD} *wrky33* mutants were generated by crossing MKK4^{DD} with *fmo1*, *ald1*, and *wrky33*. The *wrky33 sid2* double mutant was generated by crossing *wrky33-2* with *sid2-2*. The primers and methods used for mutant genotyping are listed in Supplemental Table 1.

Bacterial cultivation and inoculation

Pseudomonas syringae pv. *tomato* DC3000 harboring empty vector (*Pto*) or AvrRpt2 (*Pto* AvrRpt2) was cultivated as described (Tsuda et al., 2013). Bacterial cells were washed with H_2O, diluted to the appropriate density, and infiltrated into *A. thaliana* leaves using a needleless syringe. Similarly, *Pseudomonas syringae* pv. *maculicola* ES4326 (now classified as *Pseudomonas cannabina* pv. *alisalensis* ES4326), carrying either none transgene (*Pma*), *avrRpm1* (*Pma* AvrRpm1), or the *luxCDABE* operon of *Photorhabdus luminescens* (*Pma lux*) were grown in King's B medium containing 50 µg/ml rifampicin. For *Pma AvrRpm1* 15 µg/ml tetracycline and for *Pma lux* 50 µg/ml kanamycin were additionally added to the medium. Bacteria from overnight cultures were washed three times with 10 mM $MgCl_2$ before adjusting to the appropriate density.

Bacterial growth assay

To induce SAR with *Pto* or *Pto* AvrRpt2, bacterial suspension was infiltrated into three local leaves of 4-week-old *A. thaliana* plants. Sterilized water was infiltrated as mock control. Systemic leaves were inoculated with *Pto* 24 h post local infiltration. The bacterial titer in systemic leaves was determined 2 days post systemic infiltration. For

Pma-induced SAR, three local leaves of 4-5 week old Arabidopsis plants were infiltrated with either mock (10 mM $MgCl_2$) or *Pma*. Two days after treatment, three systemic leaves were infiltrated with *Pma lux*. Bacterial growth in systemic leaves was assessed two days post systemic infiltration via luminescence as described in Hartmann et al. (2017). To assess Pip-induced resistance to *Pma*, plants were watered with 10 ml of 1 mM Pip or water one day prior to infiltration of three rosette leaves with *Pma lux* as described in (Navarova et al., 2012). Log_{10}-transformed colony-forming units (cfu) per cm^2 leaf surface area or relative luminescence light units (rlu) per cm^2 were calculated and the following model was fit to the data; $CFU_{gyr} = GY_{gy}+R_r+e_{gyr}$, where GY, genotype:treatment interaction, and random factors; R, biological replicate; e, residual. The mean estimates of the fixed effects were used as the modeled bacterial titers and compared by two-tailed t-test.

RNA isolation and quantitative RT-PCR analysis

Total RNA was isolated from plant samples using TRIzol reagent (Thermo Fisher Scientific) following the manufacturer's instructions. Five microgram of total RNA were reverse transcribed using SuperScript II first-strand synthesis system (Thermo Fisher Scientific) with an oligo(dT) primer. Real-time DNA amplification was monitored using Bio-Rad iQ5 optical system software (Bio-Rad). The expression level of genes of interest was normalized to that of the endogenous reference gene *ACTIN2*. Primers used are listed in Supplemental Table 1. The following models were fit to the relative Ct value data compared to *ACTIN2*: $Ct_{gyr} = GY_{gy}+R_r+e_{gyr}$, where GY, genotype:treatment interaction, and random factors; R, biological replicate; e, residual; $Ct_{ytr} = YT_{yt}+R_r+e_{ytr}$, where YT, treatment:time interaction; $Ct_{gytr} = GYT_{gyt}+R_r+e_{gytr}$, where GYT, genotype:treatment:time interaction. The mean estimates of the fixed effects were used as the modeled relative Ct values, visualized as the relative log_2 expression values and compared by two-tailed t-test.

Metabolite quantification

Determination of pipecolic acid levels in leaves was performed using a protocol detailed in (Navarova et al., 2012) using GC/MS-based analysis following propyl chloroformate derivatisation. Camalexin was determined by a method based on vapor-

phase extraction and GC/MS analysis of metabolites as described previously (Attaran et al., 2009; Navarova et al., 2012). Determination of N-hydroxypipecolic acid levels in leaves was performed using a protocol detailed in (Hartmann et al., 2018) using GC/MS-analysis of leaf extracts after trimethylsilylation of analytes with N-methyl-N-trimethylsilyltrifluoroacetamide.

Growth suppression and MAP kinase assay

A. thaliana seeds were germinated on ½ MS plates (0.5 x MS salt, 1% w/v sucrose, 0.8% agar), and the 3-day-old seedlings with similar size were transferred on ½ MS plate with or without 1 µM L-pipecolic acid (Sigma), D-pipecolic acid (Sigma), or 1 µM flg22. Primary root length was measured seven days after the transfer. MAP kinase assays were performed as described previously (Lee and Ellis, 2007). Briefly, ten-day-old seedlings were transferred to a 12-well plates (3 seedlings per well) containing 2 ml of liquid MS medium with water (mock), 1 µM L-pipecolic acid, 1 µM D-pipecolic acid, and 1 µM flg22. Seedlings were frozen in liquid nitrogen at the indicated time points. The frozen seedlings were ground in liquid nitrogen and homogenized in MPK extraction buffer (100 mM HEPES, pH 7.5, 5 mM EDTA, 5 mM EGTA, 2 mM DTT, protease inhibitor cocktail (Roche Applied Science, Indianapolis, IN, USA) and phosphatase inhibitor cocktail (Roche Applied Science)). The supernatant was collected after centrifugation at 12000 rpm for 30 min at 4°C. The protein concentration was determined using a Bradford assay (BIO-RAD, Hercules, CA, USA) with bovine serum albumin as a standard. Five micrograms of protein was separated in a 12% SDS-PAGE. Immunoblot analysis was performed using anti-phospho-p44/42 MAPK (α-pTEpY, 1:5000, Cell Signaling Technology) as the primary antibody, and peroxidase-conjugated goat anti-rabbit IgG (1:20,000, Sigma) as the secondary antibody.

Chromatin Immunoprecipitation (ChIP)-qPCR

Four-week-old Col-0 and *Pwrky33:WRKY33-HA* plants were infiltrated with *Pto* AvrRpt2 (OD=0.001) or mock and the samples were collected at 24 h post infiltration. ChIP assay was performed as described previously (Yamaguchi et al., 2014) using

rabbit polyclonal anti-HA antibody. *ALD1* specific primers described in Supplemental Table 1 were used for qPCR analysis as described above.

Statistical analyses

Statistical analysis was performed using the mixed linear model function (lmer) implemented in the package lme4 in the R environment. When appropriate, raw data were log transformed to meet the assumptions of the mixed linear model. For the t-tests, the standard errors were calculated using the variance and covariance values obtained from the model fitting. The Benjamini-Hochberg method was applied to correct for multiple hypothesis testing when all pairwise comparisons of the mean estimates were made.

Accession Numbers

The accession numbers for the genes discussed in this article are as follows: At2g14610 (*PR1*), AT2G19190 (*FRK1*), AT1G74710 (*SID2*), AT1G19250 (*FMO1*), AT2G13810 (*ALD1*), AT2G38470 (*WRKY33*), AT1G64280 (*NPR1*), AT1G51660 (*MKK4*), AT3G45650 (*MPK3*), AT2G43790 (*MPK6*), AT3G18780 (*ACTIN2*).

Supplemental Data

Supplemental Figure 1. Local DEX application does not activate systemic activation of GVG system.

Supplemental Figure 2. *Pto* AvrRpt2-triggered SAR requires *ALD1*.

Supplemental Figure 3. SA and *WRKY33* contribute to SAR triggered by *Pto* infection.

Supplemental Figure 4. MAPK activation and camalexin accumulation by *Pma* infection.

Supplemental Figure 5. Pipecolic acid triggers transient MAPK activation.

Supplemental Table 1. Primers used in this study.

Acknowledgements

We thank Dr. Imre Somssich for *wrky33*, *Pwrky33:WRKY33-HA* mutants. This work was supported by the Max Planck Society and a Deutsche Forschungsgemeinschaft grant SFB670 for K.T., and a grant to J.Z. by the German Research Foundation (ZE467/6-1). Y.W. was supported by Max Planck Society and Alexander von Humboldt-Foundation.

Author contributions

YW, JZ, KT conceived and designed the experiments; YW, SS, JW, PY, ACD performed experiments; YW, JZ, and KT analyzed the data; YW, SS, JZ and KT wrote the paper. All authors commented on the manuscript.

Conflict of interest

The authors declare no competing financial interests.

Figure legends

Figure 1. MAPK-mediated SAR is largely independent of SA. (A) and **(C)** Expression levels of *PR1*, *FRK1*, and *ALD1* relative to *ACTIN2* in 4-week-old leaves determined by RT-qPCR. Leaves of DEX-inducible GUS (GUS), MKK4^{DD}, and MKK4^{DD} *sid2* plants were harvested 24 h after infiltration with 1 μM DEX or mock **(A)** and of Col-0 and *sid2* 24 h after infiltration with *Pto* AvrRpt2 (OD_{600}=0.001) or mock **(C)**. **(B)** and **(D)** Bacterial titers in systemic leaves. Primary leaves of Col-0, *sid2*, GUS, MKK4^{DD}, and MKK4^{DD} *sid2* were infiltrated with 1 μM DEX or mock **(B)** and of Col-0 and *sid2* with *Pto* AvrRpt2 (OD_{600}=0.001) or mock **(D)**. After 1 day, systemic leaves were infiltrated with *Pto* (OD_{600}=0.001), and bacterial titers in the systemic leaves were measured at 2 days post systemic infection. **(A)** to **(D)** Bars represent means and standard errors calculated from three independent experiments each with three biological replicates using a mixed linear model. (**, P < 0.01; two-tailed Student's t-tests. n.s., not significant).

Figure 2. MAPK-mediated SAR requires *ALD1*. (A) Bacterial titers in systemic leaves of GUS, MKK4^{DD}, MKK4^{DD} *sid2*, MKK4^{DD} *fmo1*, MKK4^{DD} *ald1*, and MKK4^{DD} *npr1*. Primary leaves were infiltrated with 1 μM DEX or mock. After 1 day, systemic leaves were infiltrated with *Pto* (OD_{600}=0.001), and bacterial titers in the systemic leaves were measured at 2 days post systemic infection. Bars represent means and standard errors calculated from three independent experiments each with three biological replicates using a mixed linear model. ** indicates significant difference from Mock (P < 0.01; two-tailed Student's t-tests). n.s., not significant **(B**) Phosphorylation of MPK3 and MPK6, and protein level accumulation of MKK4^{DD}, MPK3, and MPK6 in local leaves of MKK4^{DD}, MKK4^{DD} *sid2*, MKK4^{DD} *fmo1*, MKK4^{DD} *ald1*, MKK4^{DD} *npr1*, and MKK4^{DD} *wrky33* plants at the indicated time points after infiltration with 1 μM DEX. **(C)** Pipecolic acid and N-hydroxypipecolic acid levels in local leaves of MKK4^{DD} plants infiltrated with 1 μM DEX or mock at the indicated time points. N.D. indicates under the detection limit. Bars represent means and standard errors calculated from three independent experiments. ** indicates significant difference from 0 hpi (P < 0.01; two-tailed Student's t-tests).

Figure 3. MPK3 and MPK6 positively regulate Pip accumulation during *Pto* AvrRpt2 infection. (A) Bacterial titers in systemic leaves of Col-0, *mpk3*, *mpk6*, *sid2*, *mpk3 sid2*, and *mpk6 sid2*. Primary leaves were infiltrated with *Pto* AvrRpt2 (OD_{600}=0.001) or mock. After 1 day, systemic leaves were infiltrated with *Pto* (OD_{600}=0.001), and bacterial titers were measured at 2 days post systemic infection. Bars represent means and standard errors calculated from six independent experiments each with four biological replicates using a mixed linear model. **(B)** Expression of *PR1*, *ALD1*, and *FMO1* in Col-0, *mpk3*, *mpk6*, *sid2*, *mpk3 sid2*, and *mpk6 sid2* at 24 h post infiltration with *Pto* AvrRpt2 (OD_{600}=0.001) or mock determined by RT-qPCR. Bars represent means and standard errors of the $\log_2$ expression levels relative to *ACTIN2* calculated from three independent experiments each with three biological replicates using a mixed linear model. **(C)** Local Pip accumulation in leaves of Col-0, *mpk3*, *mpk6*, *sid2*, *mpk3 sid2*, and *mpk6 sid2* at 24 h post infiltration with *Pto* AvrRpt2 (OD_{600}=0.001) or mock. Bars represent means and standard errors of four independent biological replicates. Statistical differences were calculated using a mixed linear model followed by two-tailed Student's t-tests. **(A)** to **(C)** Different letters above the bars denote statistically significant differences (adjusted $P < 0.05$). Uppercase letters indicate comparisons between genotypes for SAR effects.

Figure 4. MAPK-mediated Pip accumulation and SAR are compromised in *wrky33*. (A) and **(D)** *PR1*, *ALD1*, and *FMO1* expression in leaves of $MKK4^{DD}$ and $MKK4^{DD}$ *wrky33* at 24 h after infiltration with 1 µM DEX or mock determined by RT-qPCR **(A)** and of Col-0, *wrky33*, *sid2* and *wrky33 sid2* at 24 h after infiltration with *Pto* AvrRpt2 (OD_{600}=0.001) or mock **(D)**. Bars represent means and standard errors calculated from two independent experiments each with three biological replicates using a mixed linear model. **(B)** and **(E)** Pip accumulation in leaves of $MKK4^{DD}$ and $MKK4^{DD}$ *wrky33* at 24 h after infiltration with 1 µM DEX **(B)** and of Col-0, *wrky33*, *sid2* and *wrky33 sid2* at 7 h, 12 h, and 24 h after infiltration with *Pto* AvrRpt2 (OD_{600}=0.001) or mock **(E)**. Bars represent means and standard errors calculated from five **(B)** or three **(E)** independent biological replicates. **(E)** Statistical differences were calculated using a mixed linear model followed by two-tailed Student's t-tests. **(C)** and **(F)** Bacterial titers in systemic leaves of $MKK4^{DD}$ and $MKK4^{DD}$ *wrky33* **(C)** and of Col-0, *wrky33*, *sid2* and *wrky33 sid2* **(F)**. Primary leaves were infiltrated with 1 µM DEX or

mock **(C)** and with *Pto* AvrRpt2 (OD_{600}=0.001) or mock **(F)**. After 1 day, systemic leaves were infiltrated with *Pto* (OD_{600}=0.001), and bacterial titers in the systemic leaves were measured at 2 days post systemic infection. Bars represent means and standard errors calculated from at least four independent experiments each with three biological replicates using a mixed linear model. **(A)** to **(F)** Different letters above the bars denote statistically significant differences (adjusted P < 0.05). **, P < 0.01; two-tailed Student's t-tests. n.s., not significant.

Figure 5. SA and *WRKY33* contribute to SAR triggered by *Pma* infection. **(A)** and **(B)** Bacterial titers in systemic leaves of Col-0, *mpk3*, *mpk6*, *sid2*, *mpk3 sid2*, and *mpk6 sid2* **(A)** and of Col-0 and *wrky33* **(B)**. Primary leaves were infiltrated with *Pma* (OD_{600}=0.005) or mock. After 2 days, systemic leaves were infiltrated with *Pma lux* (OD_{600}=0.001), and the bioluminescence of *Pma* lux was determined at 60 h post systemic infection. Bars represent means and standard errors calculated from at least four independent experiments each with three biological replicates using a mixed linear model. **(C)** Pip accumulation in local leaves at 24 h and systemic leaves at 48h, and N-hydroxypipecolic acid accumulation in local leaves of Col-0, *mpk3*, *mpk6*, and *wrky33* at 24 h post infiltration with *Pma* (OD_{600}=0.001) or mock (10 mM $MgCl_2$). Bars represent means and standard errors of three biological replicates. N.D. indicates under the detection limit. Statistical differences were calculated using a mixed linear model followed by two-tailed Student's t-tests. **(A)** to **(C)** Different letters above the bars denote statistically significant differences (adjusted P < 0.05). Uppercase letters indicate comparisons between genotypes for SAR effects. **, P < 0.01; two-tailed Student's t-tests.

Figure 6. WRKY33 binds to *ALD1* promoter. (A) Schematic diagram of *ALD1* promoter. The vertical black bars represent W-boxes. The horizontal lines show the regions amplified by different qPCR primers. **(B)** Protein accumulation of WRKY33 in WRYK33-HA *wrky33* plants after infiltration with *Pto* AvrRpt2 (OD_{600}=0.001) or mock at the indicated time points visualized by immunoblotting using anti-HA antibody. Ponceau S-stained RuBisCo is shown as a loading control. **(C)** ChIP-qPCR was performed using Col-0 and WRYK33-HA *wrky33* at 1 day after infiltration with *Pto* AvrRpt2 (OD_{600}=0.001). Bars represent means and standard errors of the fold

enrichment relative to Col-0 (set to 1), calculated from three independent biological replicates (**, P-value < 0.01, two-tailed Student's t-tests. n.s., not significant).

Figure 7. Pip triggers MAPK activation. (A) Col-0 and *bak1 bkk1* plants were grown on ½ MS medium containing 1 µM flg22, 1 µM L-Pip, 1 µM D-Pip, or mock, and primary root length was measured at 10 days old. Bars represent means and standard errors calculated from four independent biological replicates using a mixed linear model. **(B)** MAPK activation in 10-day-old seedlings of Col-0 and *bak1 bkk1*. Seedlings were collected at 15 min after the treatment with 1 µM flg22, 1 µM L-Pip, 1 µM D-Pip, or mock. **(C)** and **(D)** MAPK activation in leaves of 4-week-old Col-0, *wrky33*, *ald1*, and *fmo1* after infiltration with *Pto* AvrRpt2 (OD_{600}=0.001), and samples were collected at the indicated time points. **(B)** to **(D)** Proteins were detected by immunoblotting using the indicated antibodies. Ponceau S-stained RuBisCo is shown as a loading control. Similar results were observed in three independent experiments. **(E)** Bacterial titers in leaves of Col-0, *mpk3*, *mpk6*, *wrky33*, and *bak1 bkk1*. Five-week-old plants were supplied with 10 ml of 1 mM Pip (dosage of 10 µmol) or water via the root system. Three leaves per plant were infiltrated with *Pma lux* (OD_{600}=0.001) at 1 day post treatment, and relative luminescence light units (rlu) per cm^2 (log_{10}) were measured at 60 hours post systemic infection. Bars represent means and standard errors of at least three independent biological replicates using a mixed linear model. **(A)** and **(E)** Different letters above the bars denote statistically significant differences (adjusted P < 0.01). **(F)** Model for the immune-amplification loop consisting of MPK3/6, WRKY33, ALD1, and pipecolic acid.

References

Asai, T., Tena, G., Plotnikova, J., Willmann, M.R., Chiu, W.L., Gomez-Gomez, L., Boller, T., Ausubel, F.M., and Sheen, J. (2002). MAP kinase signalling cascade in Arabidopsis innate immunity. Nature **415,** 977-983.

Attaran, E., Zeier, T.E., Griebel, T., and Zeier, J. (2009). Methyl Salicylate Production and Jasmonate Signaling Are Not Essential for Systemic Acquired Resistance in Arabidopsis. Plant Cell **21,** 954-971.

Axtell, M.J., and Staskawicz, B.J. (2003). Initiation of RPS2-specified disease resistance in Arabidopsis is coupled to the AvrRpt2-directed elimination of RIN4. Cell **112,** 369-377.

Beckers, G.J.M., Jaskiewicz, M., Liu, Y.D., Underwood, W.R., He, S.Y., Zhang, S.Q., and Conrath, U. (2009). Mitogen-Activated Protein Kinases 3 and 6 Are Required for Full Priming of Stress Responses in Arabidopsis thaliana. Plant Cell **21,** 944-953.

Belkhadir, Y., Nimchuk, Z., Hubert, D.A., Mackey, D., and Dangl, J.L. (2004). Arabidopsis RIN4 negatively regulates disease resistance mediated by RPS2 and RPM1 downstream or independent of the NDR1 signal modulator and is not required for the virulence functions of bacterial type III effectors AvrRpt2 or AvrRpm1. Plant Cell **16,** 2822-2835.

Bernsdorff, F., Doring, A.C., Gruner, K., Schuck, S., Brautigam, A., and Zeier, J. (2016). Pipecolic Acid Orchestrates Plant Systemic Acquired Resistance and Defense Priming via Salicylic Acid-Dependent and -Independent Pathways. Plant Cell **28,** 102-129.

Bi, G., Zhou, Z., Wang, W., Li, L., Rao, S., Wu, Y., Zhang, X., Menke, F.L.H., Chen, S., and Zhou, J.M. (2018). Receptor-Like Cytoplasmic Kinases Directly Link Diverse Pattern Recognition Receptors to the Activation of Mitogen-Activated Protein Kinase Cascades in Arabidopsis. Plant Cell **30,** 1543-1561.

Birkenbihl, R.P., Diezel, C., and Somssich, I.E. (2012). Arabidopsis WRKY33 is a key transcriptional regulator of hormonal and metabolic responses toward Botrytis cinerea infection. Plant Physiol **159,** 266-285.

Birkenbihl, R.P., Kracher, B., Roccaro, M., and Somssich, I.E. (2017). Induced genome-wide binding of three Arabidopsis WRKY transcription factors during early MAMP-triggered immunity (vol 29, pg 20, 2017). Plant Cell **29,** 1175-1175.

Boller, T., and Felix, G. (2009). A Renaissance of Elicitors: Perception of Microbe-Associated Molecular Patterns and Danger Signals by Pattern-Recognition Receptors. Annual Review of Plant Biology **60,** 379-406.

Boutrot, F., and Zipfel, C. (2017). Function, Discovery, and Exploitation of Plant Pattern Recognition Receptors for Broad-Spectrum Disease Resistance. Annual Review of Phytopathology, Vol 55 **55,** 257-286.

Cao, H., Glazebrook, J., Clarke, J.D., Volko, S., and Dong, X. (1997). The Arabidopsis NPR1 gene that controls systemic acquired resistance encodes a novel protein containing ankyrin repeats. Cell **88,** 57-63.

Chanda, B., Xia, Y., Mandal, M.K., Yu, K.S., Sekine, K.T., Gao, Q.M., Selote, D., Hu, Y.L., Stromberg, A., Navarre, D., Kachroo, A., and Kachroo, P. (2011). Glycerol-3-phosphate is a critical mobile inducer of systemic immunity in plants. Nat Genet **43,** 421-+.

Chaturvedi, R., Venables, B., Petros, R.A., Nalam, V., Li, M.Y., Wang, X.M., Takemoto, L.J., and Shah, J. (2012). An abietane diterpenoid is a potent activator of systemic acquired resistance. Plant J **71,** 161-172.

Chen, Y.C., Holmes, E.C., Rajniak, J., Kim, J.G., Tang, S., Fischer, C.R., Mudgett, M.B., and Sattely, E.S. (2018). N-hydroxy-pipecolic acid is a mobile metabolite that induces systemic disease resistance in Arabidopsis. P Natl Acad Sci USA **115,** E4920-E4929.

Chinchilla, D., Zipfel, C., Robatzek, S., Kemmerling, B., Nurnberger, T., Jones, J.D.G., Felix, G., and Boller, T. (2007). A flagellin-induced complex of the receptor FLS2 and BAK1 initiates plant defence. Nature **448,** 497-U412.

Cui, H.T., Tsuda, K., and Parker, J.E. (2015). Effector-Triggered Immunity: From Pathogen Perception to Robust Defense. Annu Rev Plant Biol **66,** 487-511.

Delaney, T.P., Uknes, S., Vernooij, B., Friedrich, L., Weymann, K., Negrotto, D., Gaffney, T., Gutrella, M., Kessmann, H., Ward, E., and Ryals, J. (1994). A Central Role of Salicylic-Acid in Plant-Disease Resistance. Science **266,** 1247-1250.

Ding, P.T., Rekhter, D., Ding, Y.L., Feussner, K., Busta, L., Haroth, S., Xu, S.H., Li, X., Jetter, R., Feussner, I., and Zhang, Y.L. (2016). Characterization of a Pipecolic Acid Biosynthesis Pathway Required for Systemic Acquired Resistance. Plant Cell **28,** 2603-2615.

Ding, Y., Sun, T., Ao, K., Peng, Y., Zhang, Y., Li, X., and Zhang, Y. (2018). Opposite Roles of Salicylic Acid Receptors NPR1 and NPR3/NPR4 in Transcriptional Regulation of Plant Immunity. Cell **173,** 1454-1467 e1415.

Fu, Z.Q., and Dong, X.N. (2013). Systemic Acquired Resistance: Turning Local Infection into Global Defense. Annual Review of Plant Biology, Vol 64 **64,** 839-863.

Gomez-Gomez, L., and Boller, T. (2000). FLS2: An LRR receptor-like kinase involved in the perception of the bacterial elicitor flagellin in Arabidopsis. Mol Cell **5,** 1003-1011.

Hartmann, M., and Zeier, J. (2018). L-Lys metabolism to N-hydroxypipecolic acid: an integral immune-activating pathway in plants. Plant J, doi: 10.1111/tpj.14037.

Hartmann, M., Kim, D., Bernsdorff, F., Ajami-Rashidi, Z., Scholten, N., Schreiber, S., Zeier, T., Schuck, S., Reichel-Deland, V., and Zeier, J. (2017). Biochemical Principles and Functional Aspects of Pipecolic Acid Biosynthesis in Plant Immunity. Plant Physiol **174,** 124-153.

Hartmann, M., Zeier, T., Bernsdorff, F., Reichel-Deland, V., Kim, D., Hohmann, M., Scholten, N., Schuck, S., Brautigam, A., Holzel, T., Ganter, C., and Zeier, J. (2018). Flavin Monooxygenase-Generated N-Hydroxypipecolic Acid Is a Critical Element of Plant Systemic Immunity. Cell **173,** 456-469.

Heese, A., Hann, D.R., Gimenez-Ibanez, S., Jones, A.M.E., He, K., Li, J., Schroeder, J.I., Peck, S.C., and Rathjen, J.P. (2007). The receptor-like kinase SERK3/BAK1 is a central regulator of innate immunity in plants. P Natl Acad Sci USA **104,** 12217-12222.

Huot, B., Yao, J., Montgomery, B.L., and He, S.Y. (2014). Growth-Defense Tradeoffs in Plants: A Balancing Act to Optimize Fitness. Mol Plant **7,** 1267-1287.

Jones, J.D.G., and Dangl, J.L. (2006). The plant immune system. Nature **444,** 323-329.

Jung, H.W., Tschaplinski, T.J., Wang, L., Glazebrook, J., and Greenberg, J.T. (2009). Priming in Systemic Plant Immunity. Science **324,** 89-91.

Krol, E., Mentzel, T., Chinchilla, D., Boller, T., Felix, G., Kemmerling, B., Postel, S., Arents, M., Jeworutzki, E., Al-Rasheid, K.A.S., Becker, D., and Hedrich, R. (2010). Perception of the Arabidopsis Danger Signal Peptide 1 Involves the Pattern Recognition Receptor AtPEPR1 and Its Close Homologue AtPEPR2. J Biol Chem **285,** 13471-13479.

Lawton, K., Weymann, K., Friedrich, L., Vernooij, B., Uknes, S., and Ryals, J. (1995). Systemic acquired resistance in Arabidopsis requires salicylic acid but not ethylene. Molecular plant-microbe interactions : MPMI **8,** 863-870.

Lee, J.S., and Ellis, B.E. (2007). Arabidopsis MAPK phosphatase 2 (MKP2) positively regulates oxidative stress tolerance and inactivates the MPK3 and MPK6 MAPKs. J Biol Chem **282,** 25020-25029.

Li, G.J., Meng, X.Z., Wang, R.G., Mao, G.H., Han, L., Liu, Y.D., and Zhang, S.Q. (2012). Dual-Level Regulation of ACC Synthase Activity by MPK3/MPK6 Cascade and Its Downstream WRKY Transcription Factor during Ethylene Induction in Arabidopsis. Plos Genet **8**.

Liao, C.J., Lai, Z., Lee, S., Yun, D.J., and Mengiste, T. (2016). Arabidopsis HOOKLESS1 Regulates Responses to Pathogens and Abscisic Acid through Interaction with MED18 and Acetylation of WRKY33 and ABI5 Chromatin. Plant Cell **28,** 1662-1681.

Liu, P.P., von Dahl, C.C., and Klessig, D.F. (2011). The Extent to Which Methyl Salicylate Is Required for Signaling Systemic Acquired Resistance Is Dependent on Exposure to Light after Infection. Plant Physiol **157,** 2216-2226.

Liu, S., Ziegler, J., Zeier, J., Birkenbihl, R.P., and Somssich, I.E. (2017). Botrytis cinerea B05.10 promotes disease development in Arabidopsis by suppressing WRKY33-mediated host immunity. Plant Cell Environ **40,** 2189-2206.

Liu, S.A., Kracher, B., Ziegler, J., Birkenbihl, R.P., and Somssich, I.E. (2015). Negative regulation of ABA signaling by WRKY33 is critical for Arabidopsis immunity towards Botrytis cinerea 2100. Elife **4**.

Liu, Y.D., and Zhang, S.Q. (2004). Phosphorylation of 1-aminocyclopropane-1-carboxylic acid synthase by MPK6, a stress-responsive mitogen-activated protein kinase, induces ethylene biosynthesis in Arabidopsis. Plant Cell **16,** 3386-3399.

Mackey, D., Holt, B.F., Wiig, A., and Dangl, J.L. (2002). RIN4 interacts with Pseudomonas syringae type III effector molecules and is required for RPM1-mediated resistance in Arabidopsis. Cell **108,** 743-754.

Mackey, D., Belkhadir, Y., Alonso, J.M., Ecker, J.R., and Dangl, J.L. (2003). Arabidopsis RIN4 is a target of the type III virulence effector AvrRpt2 and modulates RPS2-mediated resistance. Cell **112,** 379-389.

Mao, G.H., Meng, X.Z., Liu, Y.D., Zheng, Z.Y., Chen, Z.X., and Zhang, S.Q. (2011). Phosphorylation of a WRKY Transcription Factor by Two Pathogen-Responsive MAPKs Drives Phytoalexin Biosynthesis in Arabidopsis. Plant Cell **23,** 1639-1653.

Meng, X.Z., and Zhang, S.Q. (2013). MAPK Cascades in Plant Disease Resistance Signaling. Annu Rev Phytopathol **51,** 245-266.

Mishina, T.E., and Zeier, J. (2006). The Arabidopsis flavin-dependent monooxygenase FMO1 is an essential component of biologically induced systemic acquired resistance. Plant Physiol **141,** 1666-1675.

Navarova, H., Bernsdorff, F., Doring, A.C., and Zeier, J. (2012). Pipecolic Acid, an Endogenous Mediator of Defense Amplification and Priming, Is a Critical Regulator of Inducible Plant Immunity. Plant Cell **24,** 5123-5141.

Nawrath, C., and Metraux, J.P. (1999). Salicylic acid induction-deficient mutants of Arabidopsis express PR-2 and PR-5 and accumulate high levels of camalexin after pathogen inoculation. Plant Cell **11,** 1393-1404.

Pajerowska-Mukhtar, K.M., Emerine, D.K., and Mukhtar, M.S. (2013). Tell me more: roles of NPRs in plant immunity. Trends Plant Sci **18,** 402-411.

Park, S.W., Kaimoyo, E., Kumar, D., Mosher, S., and Klessig, D.F. (2007). Methyl salicylate is a critical mobile signal for plant systemic acquired resistance. Science **318,** 113-116.

Ren, D., Liu, Y., Yang, K.Y., Han, L., Mao, G., Glazebrook, J., and Zhang, S. (2008). A fungal-responsive MAPK cascade regulates phytoalexin biosynthesis in Arabidopsis. Proc Natl Acad Sci U S A **105,** 5638-5643.

Ren, D.T., Yang, H.P., and Zhang, S.Q. (2002). Cell death mediated by MAPK is associated with hydrogen peroxide production in Arabidopsis. J Biol Chem **277,** 559-565.

Ross, A., Yamada, K., Hiruma, K., Yamashita-Yamada, M., Lu, X.L., Takano, Y., Tsuda, K., and Saijo, Y. (2014). The Arabidopsis PEPR pathway couples local and systemic plant immunity. Embo Journal **33,** 62-75.

Roux, M., Schwessinger, B., Albrecht, C., Chinchilla, D., Jones, A., Holton, N., Malinovsky, F.G., Tor, M., de Vries, S., and Zipfel, C. (2011). The Arabidopsis Leucine-Rich Repeat Receptor-Like Kinases BAK1/SERK3 and BKK1/SERK4 Are Required for Innate Immunity to Hemibiotrophic and Biotrophic Pathogens. Plant Cell **23,** 2440-2455.

Shah, J., and Zeier, J. (2013). Long-distance communication and signal amplification in systemic acquired resistance. Front Plant Sci **4,** 30.

Shan, L.B., He, P., Li, J.M., Heese, A., Peck, S.C., Nurnberger, T., Martin, G.B., and Sheen, J. (2008). Bacterial effectors target the common signaling partner

878 BAK1 to disrupt multiple MAMP receptor-signaling complexes and impede
879 plant immunity. Cell Host Microbe **4,** 17-27.
880 **Sun, T., Busta, L., Zhang, Q., Ding, P., Jetter, R., and Zhang, Y.** (2017). TGACG-
881 BINDING FACTOR 1 (TGA1) and TGA4 regulate salicylic acid and pipecolic
882 acid biosynthesis by modulating the expression of SYSTEMIC ACQUIRED
883 RESISTANCE DEFICIENT 1 (SARD1) and CALMODULIN-BINDING
884 PROTEIN 60g (CBP60g). New Phytol.
885 **Sun, T.J., Zhang, Y.X., Li, Y., Zhang, Q., Ding, Y.L., and Zhang, Y.L.** (2015). ChIP-
886 seq reveals broad roles of SARD1 and CBP60g in regulating plant immunity.
887 Nat Commun **6**.
888 **Tran, D.T.N., Chung, E.H., Habring-Muller, A., Demar, M., Schwab, R., Dangl,**
889 **J.L., Weigel, D., and Chae, E.** (2017). Activation of a Plant NLR Complex
890 through Heteromeric Association with an Autoimmune Risk Variant of Another
891 NLR. Curr Biol **27,** 1148-1160.
892 **Tsuda, K., and Katagiri, F.** (2010). Comparing signaling mechanisms engaged in
893 pattern-triggered and effector-triggered immunity. Curr Opin Plant Biol **13,**
894 459-465.
895 **Tsuda, K., Mine, A., Bethke, G., Igarashi, D., Botanga, C.J., Tsuda, Y.,**
896 **Glazebrook, J., Sato, M., and Katagiri, F.** (2013). Dual Regulation of Gene
897 Expression Mediated by Extended MAPK Activation and Salicylic Acid
898 Contributes to Robust Innate Immunity in Arabidopsis thaliana. Plos Genet **9**.
899 **Vernooij, B., Friedrich, L., Morse, A., Reist, R., Kolditzjawhar, R., Ward, E.,**
900 **Uknes, S., Kessmann, H., and Ryals, J.** (1994). Salicylic-Acid Is Not the
901 Translocated Signal Responsible for Inducing Systemic Acquired-Resistance
902 but Is Required in Signal Transduction. Plant Cell **6,** 959-965.
903 **Vogel-Adghough, D., Stahl, E., Navarova, H., and Zeier, J.** (2013). Pipecolic acid
904 enhances resistance to bacterial infection and primes salicylic acid and
905 nicotine accumulation in tobacco. Plant signaling & behavior **8,** e26366.
906 **Wang, H.C., Ngwenyama, N., Liu, Y.D., Walker, J.C., and Zhang, S.Q.** (2007).
907 Stomatal development and patterning are regulated by environmentally
908 responsive mitogen-activated protein kinases in Arabidopsis. Plant Cell **19,** 63-
909 73.

Wang, L., Tsuda, K., Truman, W., Sato, M., Nguyen, L.V., Katagiri, F., and Glazebrook, J. (2011). CBP60g and SARD1 play partially redundant critical roles in salicylic acid signaling. Plant J **67,** 1029-1041.

Wildermuth, M.C., Dewdney, J., Wu, G., and Ausubel, F.M. (2001). Isochorismate synthase is required to synthesize salicylic acid for plant defence. Nature **414,** 562-565.

Wu, Y., Zhang, D., Chu, J.Y., Boyle, P., Wang, Y., Brindle, I.D., De Luca, V., and Despres, C. (2012). The Arabidopsis NPR1 Protein Is a Receptor for the Plant Defense Hormone Salicylic Acid. Cell Reports **1,** 639-647.

Xu, J., Meng, J., Meng, X.Z., Zhao, Y.T., Liu, J.M., Sun, T.F., Liu, Y.D., Wang, Q.M., and Zhang, S.Q. (2016). Pathogen-Responsive MPK3 and MPK6 Reprogram the Biosynthesis of Indole Glucosinolates and Their Derivatives in Arabidopsis Immunity. Plant Cell **28,** 1144-1162.

Yamada, K., Yamashita-Yamada, M., Hirase, T., Fujiwara, T., Tsuda, K., Hiruma, K., and Saijo, Y. (2016). Danger peptide receptor signaling in plants ensures basal immunity upon pathogen-induced depletion of BAK1. Embo Journal **35,** 46-61.

Yamaguchi, N., Winter, C.M., Wu, M.F., Kwon, C.S., William, D.A., and Wagner, D. (2014). PROTOCOLS: Chromatin Immunoprecipitation from Arabidopsis Tissues. The Arabidopsis book **12,** e0170.

Yamaguchi, Y., Huffaker, A., Bryan, A.C., Tax, F.E., and Ryan, C.A. (2010). PEPR2 Is a Second Receptor for the Pep1 and Pep2 Peptides and Contributes to Defense Responses in Arabidopsis. Plant Cell **22,** 508-522.

Yu, X., Feng, B.M., He, P., and Shan, L.B. (2017). From Chaos to Harmony: Responses and Signaling upon Microbial Pattern Recognition. Annual Review of Phytopathology, Vol 55 **55,** 109-137.

Zeier, J. (2013). New insights into the regulation of plant immunity by amino acid metabolic pathways. Plant Cell Environ **36,** 2085-2103.

Zhang, X.X., Dodds, P.N., and Bernoux, M. (2017). What Do We Know About NOD-Like Receptors in Plant Immunity? Annual Review of Phytopathology, Vol 55 **55,** 205-229.

Zhang, Y.X., Xu, S.H., Ding, P.T., Wang, D.M., Cheng, Y.T., He, J., Gao, M.H., Xu, F., Li, Y., Zhu, Z.H., Li, X., and Zhang, Y.L. (2010). Control of salicylic acid synthesis and systemic acquired resistance by two members of a plant-

944 specific family of transcription factors. P Natl Acad Sci USA **107,** 18220-
945 18225.
946 **Zheng, Z.Y., Abu Qamar, S., Chen, Z.X., and Mengiste, T.** (2006). Arabidopsis
947 WRKY33 transcription factor is required for resistance to necrotrophic fungal
948 pathogens. Plant J **48,** 592-605.
949 **Zhou, M., Lu, Y., Bethke, G., Harrison, B.T., Hatsugai, N., Katagiri, F., and**
950 **Glazebrook, J.** (2017). WRKY70 prevents axenic activation of plant immunity
951 by direct repression of SARD1. New Phytol.
952 **Zimmerli, L., Jakab, C., Metraux, J.P., and Mauch-Mani, B.** (2000). Potentiation of
953 pathogen-specific defense mechanisms in Arabidopsis by beta-aminobutyric
954 acid. P Natl Acad Sci USA **97,** 12920-12925.
955 **Zipfel, C., Robatzek, S., Navarro, L., Oakeley, E.J., Jones, J.D.G., Felix, G., and**
956 **Boller, T.** (2004). Bacterial disease resistance in Arabidopsis through flagellin
957 perception. Nature **428,** 764-767.

958

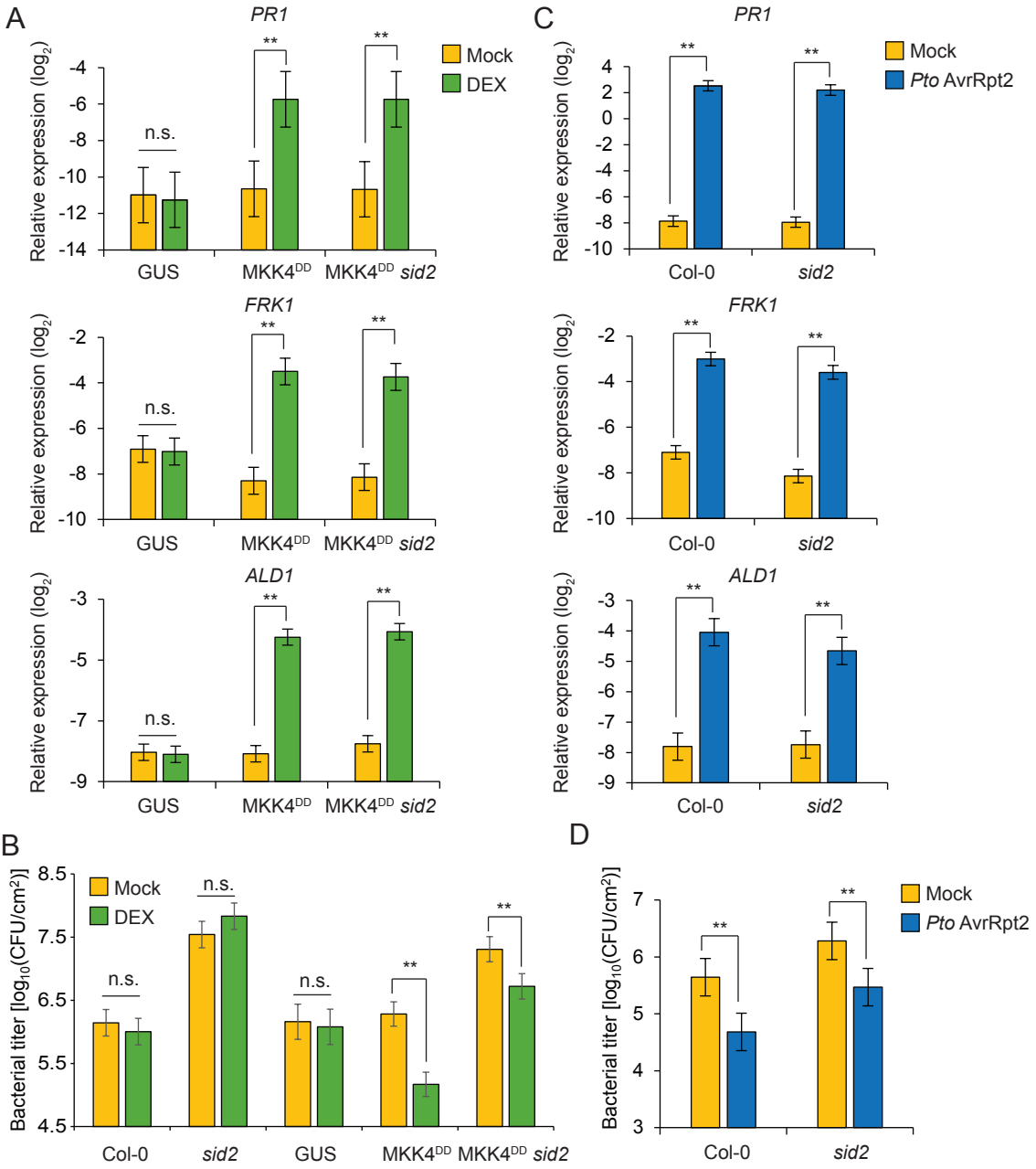

Figure 1. MAPK-mediated SAR is largely independent of SA. (A) and **(C)** Expression levels of *PR1*, *FRK1*, and *ALD1* relative to *ACTIN2* in 4-week-old leaves determined by RT-qPCR. Leaves of DEX-inducible GUS (GUS), MKK4^{DD}, and MKK4^{DD} *sid2* plants were harvested 24 h after infiltration with 1 µM DEX or mock **(A)** and of Col-0 and *sid2* 24 h after infiltration with *Pto* AvrRpt2 (OD_{600}=0.001) or mock **(C)**. **(B)** and **(D)** Bacterial titers in systemic leaves. Primary leaves of Col-0, *sid2*, GUS, MKK4DD, and MKK4DD *sid2* were infiltrated with 1 µM DEX or mock **(B)** and of Col-0 and *sid2* with *Pto* AvrRpt2 (OD_{600}=0.001) or mock **(D)**. After 1 day, systemic leaves were infiltrated with *Pto* (OD_{600}=0.001), and bacterial titers in the systemic leaves were measured at 2 days post systemic infection. **(A)** to **(D)** Bars represent means and standard errors calculated from three independent experiments each with three biological replicates using a mixed linear model. (**, P < 0.01; two-tailed Student's t-tests. n.s., not significant).

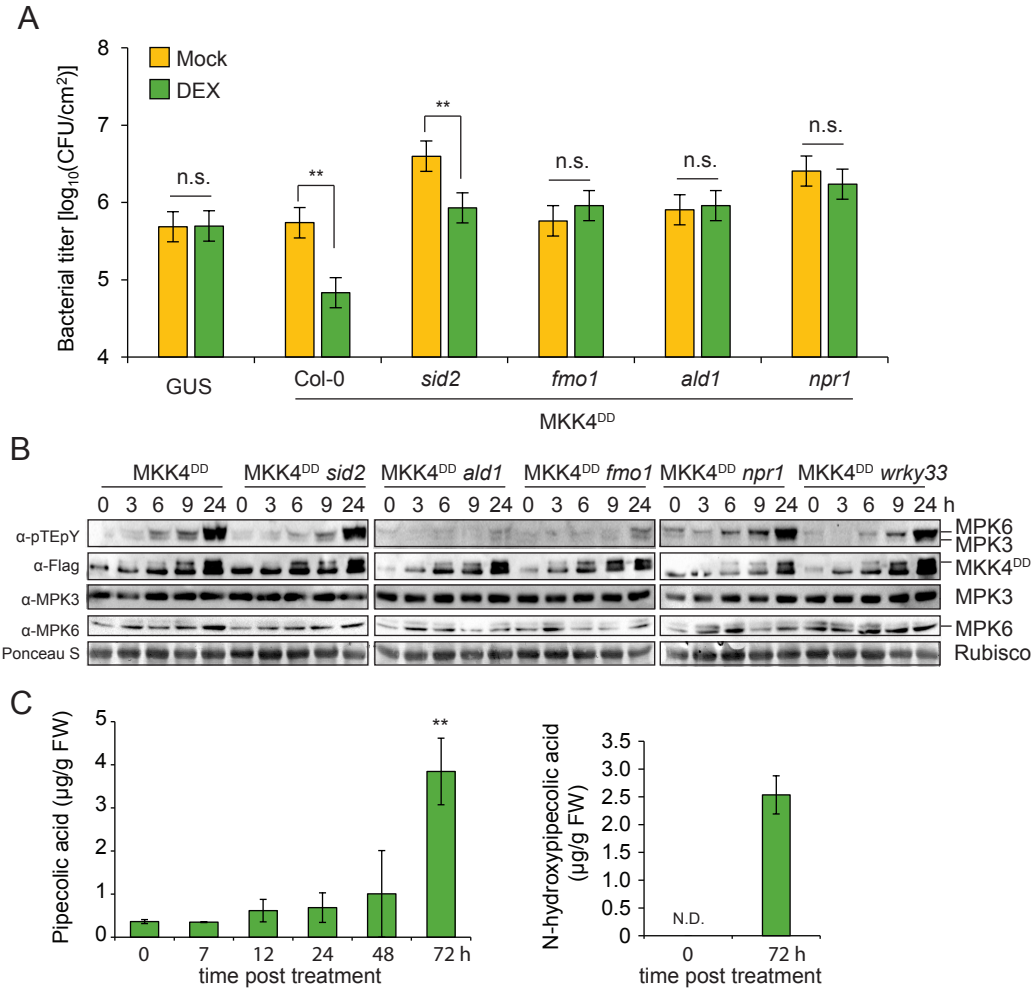

Figure 2. MAPK-mediated SAR requires *ALD1*. (A) Bacterial titers in systemic leaves of GUS, MKK4^{DD}, MKK4^{DD} *sid2*, MKK4^{DD} *fmo1*, MKK4^{DD} *ald1*, and MKK4^{DD} *npr1*. Primary leaves were infiltrated with 1 μM DEX or mock. After 1 day, systemic leaves were infiltrated with *Pto* (OD_{600}=0.001), and bacterial titers in the systemic leaves were measured at 2 days post systemic infection. Bars represent means and standard errors calculated from three independent experiments each with three biological replicates using a mixed linear model. ** indicates significant difference from Mock ($P < 0.01$; two-tailed Student's t-tests). n.s., not significant **(B)** Phosphorylation of MPK3 and MPK6, and protein level accumulation of MKK4^{DD}, MPK3, and MPK6 in local leaves of MKK4^{DD}, MKK4^{DD} *sid2*, MKK4^{DD} *fmo1*, MKK4^{DD} *ald1*, MKK4^{DD} *npr1*, and MKK4^{DD} *wrky33* plants at the indicated time points after infiltration with 1 μM DEX. **(C)** Pipecolic acid and N-hydroxypipecolic acid levels in local leaves of MKK4^{DD} plants infiltrated with 1 μM DEX or mock at the indicated time points. N.D. indicates under the detection limit. Bars represent means and standard errors calculated from three independent experiments. ** indicates significant difference from 0 hpi ($P < 0.01$; two-tailed Student's t-tests).

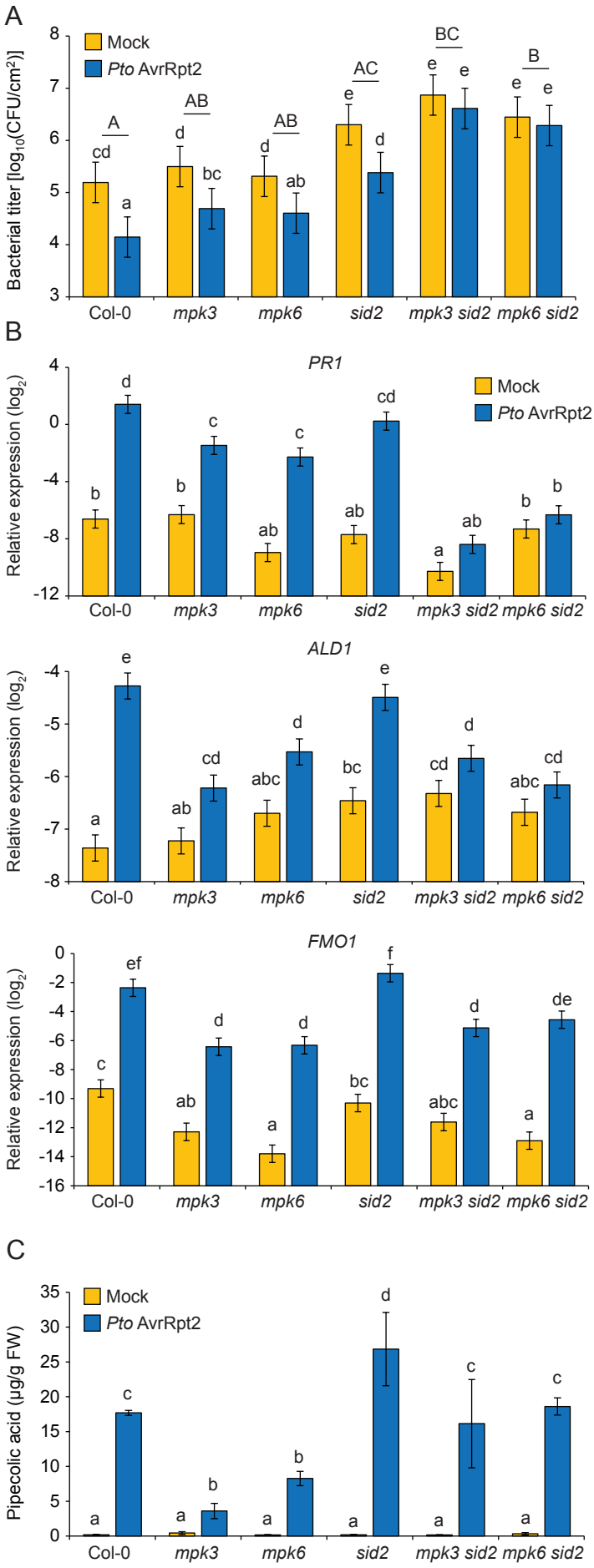

Figure 3. MPK3 and MPK6 positively regulate Pip accumulation during Pto AvrRpt2 infection. (A) Bacterial titers in systemic leaves of Col-0, *mpk3*, *mpk6*, *sid2*, *mpk3 sid2*, and *mpk6 sid2*. Primary leaves were infiltrated with *Pto* AvrRpt2 (OD_{600}=0.001) or mock. After 1 day, systemic leaves were infiltrated with Pto (OD_{600}=0.001), and bacterial titers were measured at 2 days post systemic infection. Bars represent means and standard errors calculated from six independent experiments each with four biological replicates using a mixed linear model. **(B)** Expression of *PR1*, *ALD1*, and *FMO1* in Col-0, *mpk3*, *mpk6*, *sid2*, *mpk3 sid2*, and *mpk6 sid2* at 24 h post infiltration with Pto AvrRpt2 (OD_{600}=0.001) or mock determined by RT-qPCR. Bars represent means and standard errors of the $\log_2$ expression levels relative to *ACTIN2* calculated from three independent experiments each with three biological replicates using a mixed linear model. **(C)** Local Pip accumulation in leaves of Col-0, *mpk3*, *mpk6*, *sid2*, *mpk3 sid2*, and *mpk6 sid2* at 24 h post infiltration with *Pto* AvrRpt2 (OD_{600}=0.001) or mock. Bars represent means and standard errors of four independent biological replicates. Statistical differences were calculated using a mixed linear model followed by two-tailed Student's t-tests. **(A)** to **(C)** Different letters above the bars denote statistically significant differences (adjusted $P < 0.05$). Uppercase letters indicate comparisons between genotypes for SAR effects.

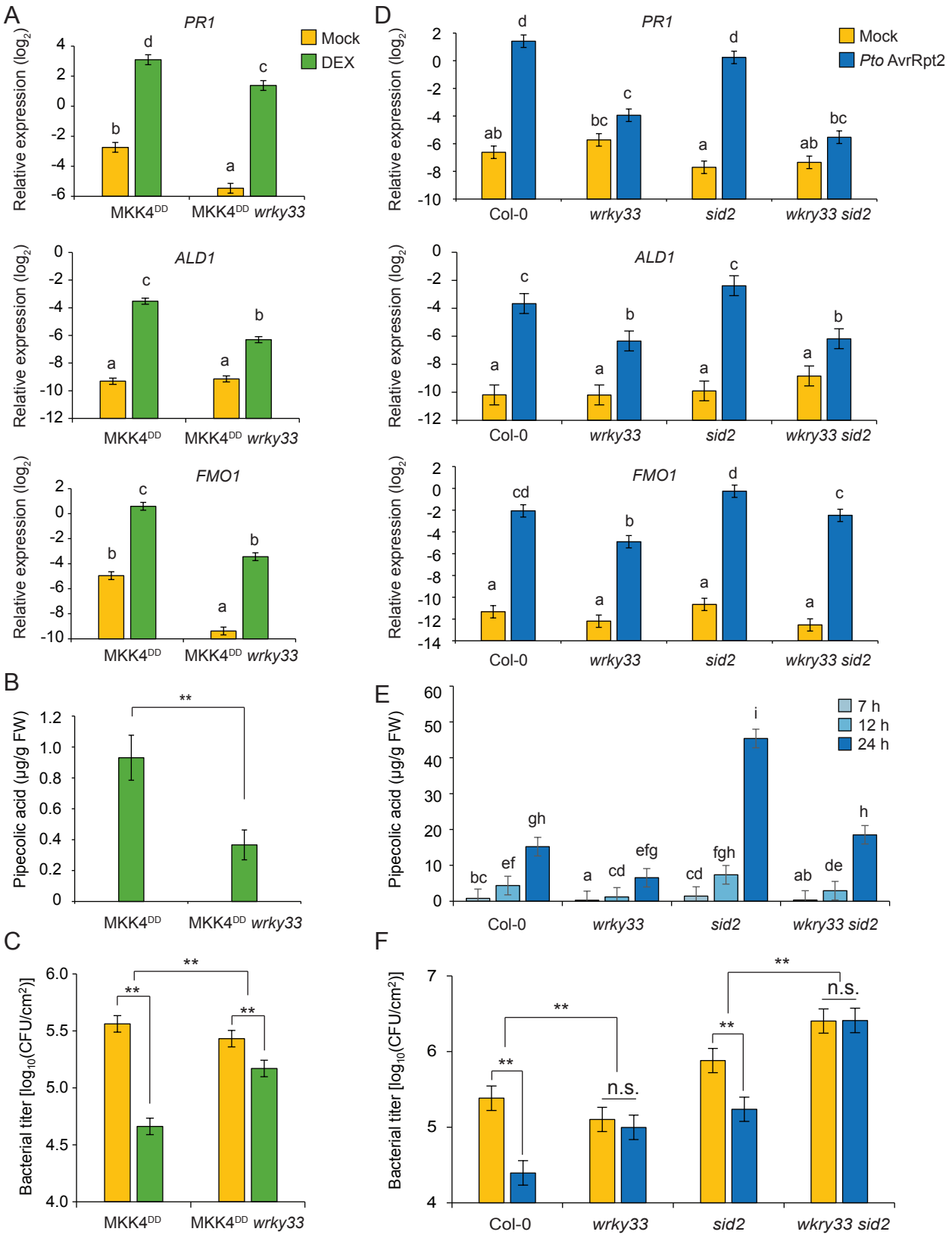

Figure 4. MAPK-mediated Pip accumulation and SAR are compromised in wrky33. (A) and **(D)** *PR1*, *ALD1*, and *FMO1* expression in leaves of MKK4^{DD} and MKK4^{DD} *wrky33* at 24 h after infiltration with 1 µM DEX or mock determined by RT-qPCR (A) and of Col-0, *wrky33*, *sid2* and *wrky33 sid2* at 24 h after infiltration with *Pto* AvrRpt2 (OD_{600}=0.001) or mock **(D)**. Bars represent means and standard errors calculated from two independent experiments each with three biological replicates using a mixed linear model. **(B)** and **(E)** Pip accumulation in leaves of MKK4^{DD} and MKK4^{DD} *wrky33* at 24 h after infiltration with 1 µM DEX **(B)** and of Col-0, *wrky33*, *sid2* and *wrky33 sid2* at 7 h, 12 h, and 24 h after infiltration with Pto AvrRpt2 (OD_{600}=0.001) or mock **(E)**. Bars represent means and standard errors calculated from five **(B)** or three **(E)** independent biological replicates. **(E)** Statistical differences were calculated using a mixed linear model followed by two-tailed Student's t-tests. **(C)** and **(F)** Bacterial titers in systemic leaves of MKK4^{DD} and MKK4^{DD} *wrky33* **(C)** and of Col-0, *wrky33*, *sid2* and *wrky33 sid2* **(F)**. Primary leaves were infiltrated with 1 µM DEX or mock **(C)** and with *Pto* AvrRpt2 (OD_{600}=0.001) or mock **(F)**. After 1 day, systemic leaves were infiltrated with Pto (OD_{600}=0.001), and bacterial titers in the systemic leaves were measured at 2 days post systemic infection. Bars represent means and standard errors calculated from at least four independent experiments each with three biological replicates using a mixed linear model. **(A)** to **(F)** Different letters above the bars denote statistically significant differences (adjusted P < 0.05). **, P < 0.01; two-tailed Student's t-tests. n.s., not significant.

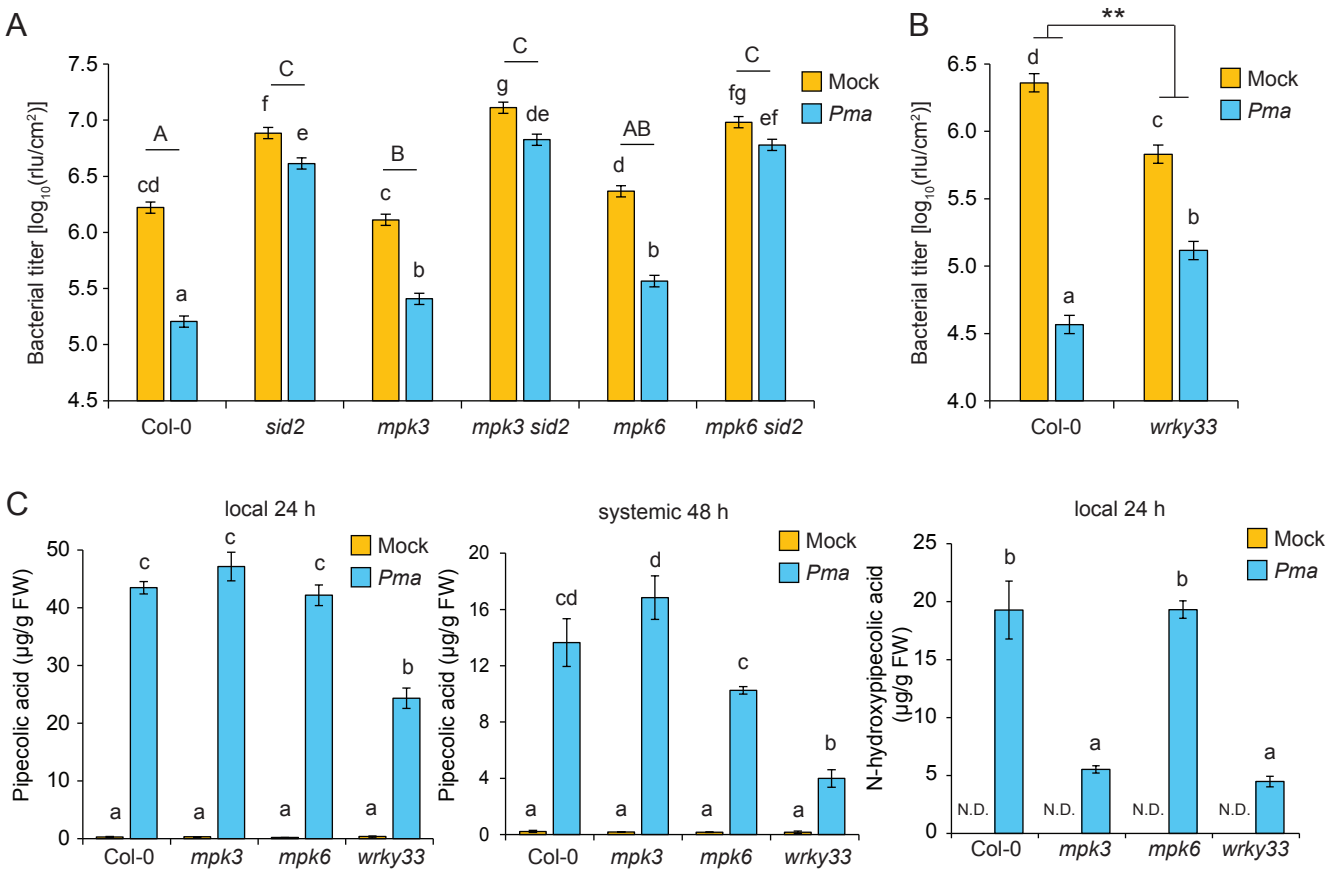

Figure 5. SA and *WRKY33* contribute to SAR triggered by *Pma* infection. **(A)** and **(B)** Bacterial titers in systemic leaves of Col-0, *mpk3*, *mpk6*, *sid2*, *mpk3 sid2*, and *mpk6 sid2* **(A)** and of Col-0 and *wrky33* **(B)**. Primary leaves were infiltrated with *Pma* (OD_{600}=0.005) or mock. After 2 days, systemic leaves were infiltrated with *Pma lux* (OD_{600}=0.001), and the bioluminescence of *Pma* lux was determined at 60 h post systemic infection. Bars represent means and standard errors calculated from at least four independent experiments each with three biological replicates using a mixed linear model. **(C)** Pip accumulation in local leaves at 24 h and systemic leaves at 48h, and N-hydroxypipecolic acid accumulation in local leaves of Col-0, *mpk3*, *mpk6*, and *wrky33* at 24 h post infiltration with *Pma* (OD_{600}=0.001) or mock (10 mM $MgCl_2$). Bars represent means and standard errors of three biological replicates. N.D. indicates under the detection limit. Statistical differences were calculated using a mixed linear model followed by two-tailed Student's t-tests. **(A)** to **(C)** Different letters above the bars denote statistically significant differences (adjusted P < 0.05). Uppercase letters indicate comparisons between genotypes for SAR effects. **, P < 0.01; two-tailed Student's t-tests.

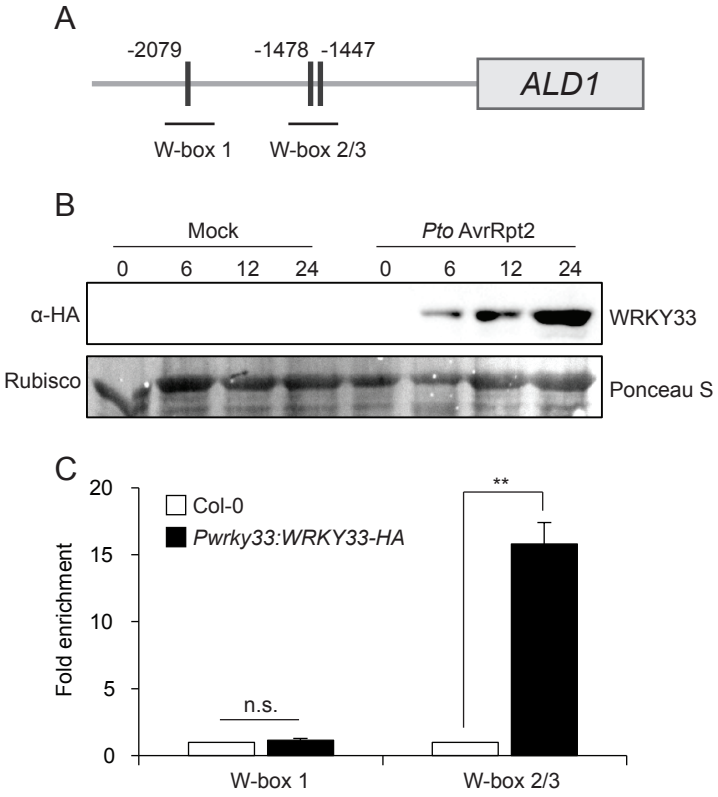

Figure 6. WRKY33 binds to *ALD1* promoter. (A) Schematic diagram of *ALD1* promoter. The vertical black bars represent W-boxes. The horizontal lines show the regions amplified by different qPCR primers. **(B)** Protein accumulation of WRKY33 in WRYK33-HA *wrky33* plants after infiltration with *Pto* AvrRpt2 (OD_{600}=0.001) or mock at the indicated time points visualized by immunoblotting using anti-HA antibody. Ponceau S-stained RuBisCo is shown as a loading control. **(C)** ChIP-qPCR was performed using Col-0 and WRYK33-HA *wrky33* at 1 day after infiltration with *Pto* AvrRpt2 (OD_{600}=0.001). Bars represent means and standard errors of the fold enrichment relative to Col-0 (set to 1), calculated from three independent biological replicates (**, P-value < 0.01, two-tailed Student's t-tests. n.s., not significant).

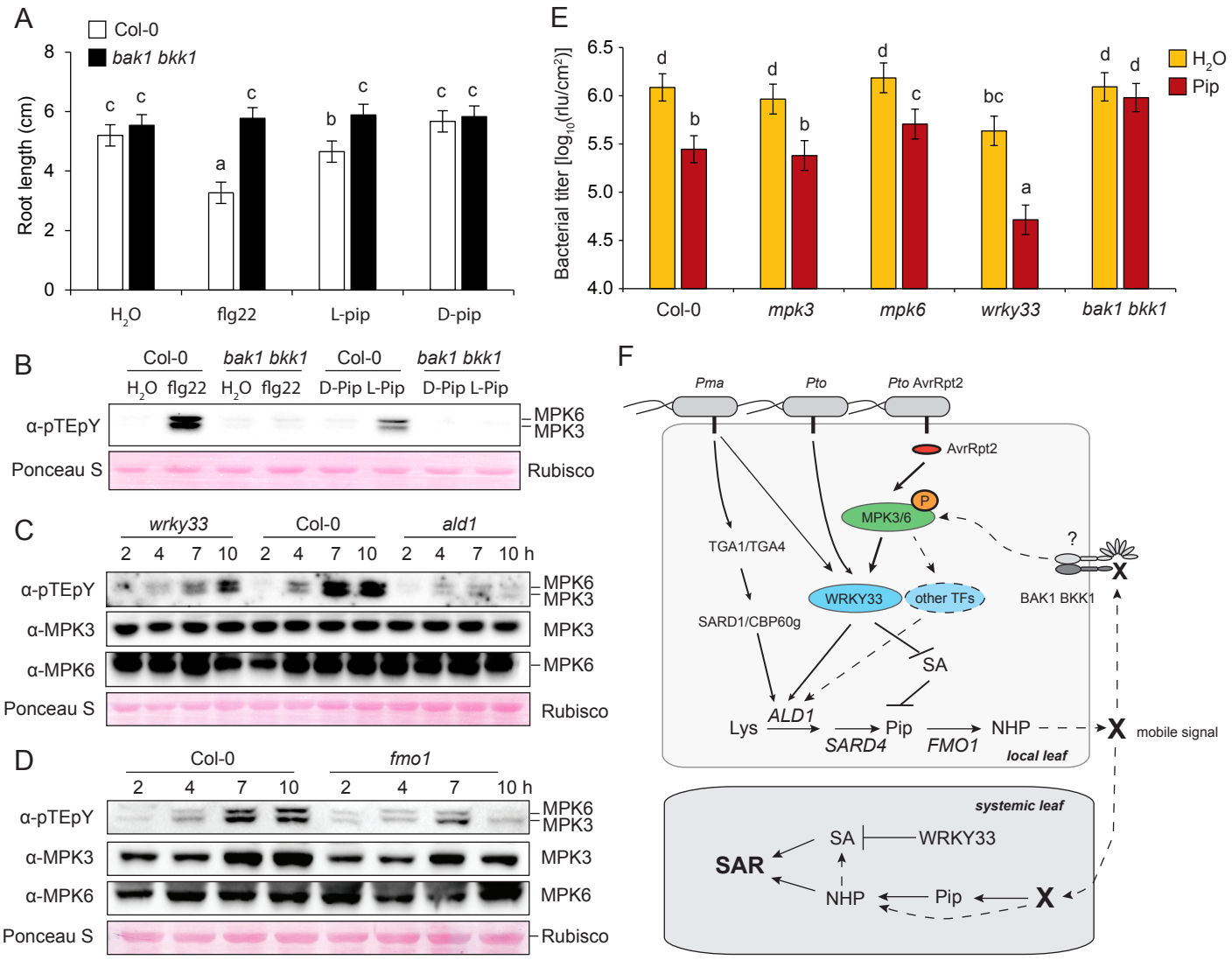

Figure 7. Pip triggers MAPK activation. (A) Col-0 and *bak1 bkk1* plants were grown on ½ MS medium containing 1 µM flg22, 1 µM L-Pip, 1 µM D-Pip, or mock, and primary root length was measured at 10 days old. Bars represent means and standard errors calculated from four independent biological replicates using a mixed linear model. **(B)** MAPK activation in 10-day-old seedlings of Col-0 and *bak1 bkk1*. Seedlings were collected at 15 min after the treatment with 1 µM flg22, 1 µM L-Pip, 1 µM D-Pip, or mock. **(C)** and **(D)** MAPK activation in leaves of 4-week-old Col-0, *wrky33*, *ald1*, and *fmo1* after infiltration with *Pto* AvrRpt2 (OD_{600}=0.001), and samples were collected at the indicated time points. **(B)** to **(D)** Proteins were detected by immunoblotting using the indicated antibodies. Ponceau S-stained RuBisCo is shown as a loading control. Similar results were observed in three independent experiments. **(E)** Bacterial titers in leaves of Col-0, *mpk3*, *mpk6*, *wrky33*, and *bak1 bkk1*. Five-week-old plants were supplied with 10 ml of 1 mM Pip (dosage of 10 µmol) or water via the root system. Three leaves per plant were infiltrated with Pma lux (OD_{600}=0.001) at 1 day post treatment, and relative luminescence light units (rlu) per cm^2 (log_{10}) were measured at 60 hours post systemic infection. Bars represent means and standard errors of at least three independent biological replicates using a mixed linear model. **(A)** and **(E)** Different letters above the bars denote statistically significant differences (adjusted P < 0.01). **(F)** Model for the immune-amplification loop consisting of MPK3/6, WRKY33, ALD1, and pipecolic acid.

A MPK3/6-WRKY33-ALD1-Pipecolic acid Regulatory Loop Contributes to Systemic Acquired Resistance

Yiming Wang, Stefan Schuck, Jingni Wu, Ping Yang, Anne-Christin Doering, Jürgen Zeier and Kenichi Tsuda

Plant Cell; originally published online September 18, 2018;
DOI 10.1105/tpc.18.00547